J. Nonlinear Var. Anal. 9 (2025), No. 1, pp. 81-110
Available online at http://jnva.biemdas.com
https://doi.org/10.23952/jnva.9.2025.1.06

A NEWTON METHOD FOR UNCERTAIN MULTIOBJECTIVE OPTIMIZATION PROBLEMS WITH FINITE UNCERTAINTY SETS

DEBDAS GHOSH[1], NAND KISHOR[1], XIAOPENG ZHAO[2,*]

[1]*Department of Mathematical Sciences, Indian Institute of Technology (BHU), Varanasi, Uttar Pradesh—221005, India*
[2]*School of Mathematical Sciences, Tiangong University, Tianjin, 300387, China*

Abstract. In this study, we investigate an uncertain multiobjective optimization problem through a set-valued optimization problem, and introduce a Newton method to find robust weakly efficient points of the considered uncertain optimization problem. We assume that the problem under consideration has uncertainty only in the objective function, and the involved uncertainty set is of finite cardinality. Also, for each uncertain scenario, the components of the objective function of the problem are assumed to be twice continuously differentiable and locally strong convex. Utilizing the concept of a *partition set* from set optimization, we formulate a class of vector optimization problems to solve the formulated set optimization problem pertaining to the considered uncertain multiobjective optimization. We derive a Newton method to solve this class of vector optimization problems that facilitates generating a sequence of points whose any limit point is a weakly robust efficient solution of the considered problem. The proposed method is found to have a local superlinear convergence rate under standard hypotheses with a regularity condition. Additionally, assuming Lipschitz continuity of the Hessian of the objective function for all scenarios, we show local quadratic convergence of the method. Finally, we provide numerical examples to discuss and illustrate the performance of the proposed method.

Keywords. Gerstewitz functional; Newton's method; Partition set; Set optimization; Uncertain optimization; Upper set order relation.

1. INTRODUCTION

Uncertain multi-objective optimization problems (UMOPs) represent a class of optimization problems that involve multiple conflicting objectives in the presence of uncertain scenarios. In many real-world problems, the objectives are uncertain due to incomplete information, imprecise data, or unpredictable factors [1, 2]. Analyzing the effects of uncertain scenarios in optimization serves several key purposes:

(i) *Trade-off analysis*: Uncertainties often introduce trade-offs between conflicting objectives. Analyzing the effects of uncertainties helps to understand the compromises and synergies between different goals, enabling decision-makers to make informed choices that align with their preferences and priorities.

*Corresponding author.
E-mail address: zhaoxiaopeng.2007@163.com (X. Zhao)
Received 2 July 2023; Accepted 5 March 2024; Published online 20 December 2024.

(ii) *Risk mitigation*: By exploring different uncertain scenarios, decision-makers can assess the potential risks associated with each scenario.
(iii) *Decision support*: The analysis of uncertain scenarios decisions not only optimize multiple objectives but also consider the resilience and adaptability of solutions under different uncertain conditions.
(iv) *Flexibility and adaptability*: Solutions prove effective across a spectrum of uncertain scenarios demonstrate greater flexibility and adaptability.

The field of uncertain (robust) optimization is expanding rapidly. For a comprehensive understanding of key concepts and applications, we recommend reviewing the research contributions of Ben-Tal, El Ghaoui, and Nemirovski [3], as well as the work by Kouvelis and Yu [4]. Kuroiwa and Lee [5] expanded the concept of min-max robustness from single-objective to multi-objective cases. A solution is called robust if it minimizes the vector of worst-case outcomes across all components. Ehrgott et al. [6] broadened this definition by replacing the objective function with a set-valued objective function. Building on this, further extensions to multi-objective robustness concepts were introduced in [7], providing methods to compute both strictly and weakly optimal solutions for UMOPs. In [8, 9], new definitions for UMOPs were proposed based on various set-order relations [10, 11]. Ide et al. [12] extended existing concepts and introduced new multi-objective robustness concepts. For additional insights, references [13, 14, 15, 16, 17, 18] offer detailed information on these developments.

This paper addresses UMOPs, which inherently involve non-deterministic parameters. To render these problems deterministic, commonly min-max counterparts are employed, which Soyster [19] introduced and rigorously studied by Ben-Tal and Nemirovski [20]. Solving UMOPs typically involves using optimization algorithms that can handle both multi-objective and uncertainty nature of the problem.

On the topic of numerical methods to solve UMOPs, the authors in [21] successfully addressed the UMOPs with a finite uncertainty set. In order to transform an uncertain optimization problem into a deterministic one, they employed the concept of an objective-wise robust counterpart. It is noteworthy that the set of all efficient solutions of the objective-wise robust counterpart is a very small subset of the whole set of robust optimal solutions of UMOPs. Thus, in this paper, we aim to derive a Newton method for UMOPs without using the objective-wise robust counterpart; in fact, we formulate a set optimization problem whose efficient points are robust efficient points of the considered UMOP. Towards the methods, we relook afresh at the min-max robust counterpart of UMOPs from the viewpoint of its set-valued optimization reformulation. After transforming UMOPs into their min-max counterparts, they resembled set-valued optimization problems. We solve this set-valued optimization problem by employing the Newton method with the upper set ordering relation, providing a robust efficient solution for UMOPs directly. We formulate a sequence of *vector optimization problems* (VOP) for the considered UMOPs by applying the concept of the *partition set*, defined in [22], to solve a set optimization problem. Our demonstration establishes that the set of weakly efficient solutions of the VOP family for a UMOP is the set of weakly robust efficient solutions of the UMOP. To address the optimality conditions of the considered UMOP, we develop a Newton algorithm that uses the partition set of the maximal elements of the set of all objective values corresponding to each scenario with respect to the ordering cone of the considered UMOP. In essence, we endeavor to comprehensively capture robust efficiency by systematically examining and partitioning the maximal elements within the uncertainty set of all objective values corresponding to each scenario. This approach seeks to provide a more exhaustive exploration of the solution space, aiming to uncover a broader set of efficient solutions that may have been overlooked in the previous methodology.

The outline of this paper is as follows. Section 2 introduces efficient solutions for multi-objective optimization problems and UMOPs. Robust efficient solutions for UMOPs are presented by using the upper-set order relation. In Section 3, building on the partition set, defined in [22], a sequence of vector optimization problems is formulated and we establish that the weakly efficient solution within this VOP family converges to the weakly robust efficient solution of the UMOP. Section 4 provides a Newton method for UMOPs, exploring its quadratic and superlinear convergence under specific hypotheses with regularity conditions. Section 5 demonstrates the method's performance through numerical examples. Finally, Section 6 concludes by summarizing the results and suggesting ideas for future research.

2. Preliminaries

A multi-objective optimization problem is a problem that has multiple objectives to be optimized simultaneously. A multi-objective optimization problem is given by

$$(\mathscr{P}) \begin{cases} \min & f(x) = (f_1(x), f_2(x), \ldots, f_m(x))^\top \\ \text{subject to} & x \in U \subseteq \mathbb{R}^n, \end{cases} \tag{2.1}$$

where $f_i : U \to \mathbb{R}$ is a real-valued function, $i = 1, 2, \ldots, m$ and $U \neq \emptyset$ is an open subset of $\mathbb{R}^n$. For a given $y = (y_1, y_2, \ldots, y_m)^\top$ in $\mathbb{R}^m$, we use the following notations throughout:

$$\mathbb{R}^m_{\geqq} = \{y \in \mathbb{R}^m : y \geqq 0\}, \text{ the nonnegative orthant of } \mathbb{R}^m.$$
$$\mathbb{R}^m_{\geq} = \{y \in \mathbb{R}^m : y \geq 0\}, \text{ where } y \geq 0 \text{ denotes } y \geqq 0 \text{ but } y \neq 0.$$
$$\mathbb{R}^m_{>} = \{y \in \mathbb{R}^m : y > 0\}, \text{ where } y > 0 \text{ means } y_j > 0 \; \forall j = 1, 2, \ldots, m.$$

Definition 2.1. [23] For a multi-objective optimization problem $(\mathscr{P})$, we call a point $\bar{x} \in U$

(i) efficient if there is no $x \in U \setminus \{\bar{x}\}$ such that $f(x) \leq f(\bar{x})$,
(ii) weakly efficient if there is no $x \in U \setminus \{\bar{x}\}$ such that $f(x) < f(\bar{x})$, and
(iii) strictly efficient if there is no $x \in U \setminus \{\bar{x}\}$, $x \neq \bar{x}$ such that $f(x) \leqq f(\bar{x})$.

In this paper, we deal with the UMOP $\mathscr{P}(\Omega) = \{\mathscr{P}(\zeta) : \zeta \in \Omega\}$ with respect to an ordering cone $C \subset \mathbb{R}^m$, where

$$\mathscr{P}(\zeta) \begin{cases} \min & F(x,\zeta) = (f_1(x,\zeta), f_2(x,\zeta), \ldots, f_m(x,\zeta))^\top \\ \text{subject to} & x \in U \subseteq \mathbb{R}^n, \end{cases} \tag{2.2}$$

and Ω is a nonempty subset of $\mathbb{R}^q$. The set Ω represents the set of uncertain (parametric) scenarios for the problem $\mathscr{P}(\Omega)$. An element in Ω is referred to as a *scenario*. Note that each element ζ of Ω gives a multi-objective problem (2.2), and thus elements of Ω, i.e., uncertain scenarios, are influential for the problem definition of $\mathscr{P}(\Omega)$.

Throughout the paper, we assume for the class of problems $\mathscr{P}(\Omega)$ that

(i) uncertainties in the problem formulation are given by finitely many ζ's, which constitute the set $\Omega \subseteq \mathbb{R}^q$. Precisely, let $\Omega = \{\zeta_1, \zeta_2, \ldots, \zeta_p\}$.

(ii) The feasible set U is independent of uncertainties, and it is a nonempty open subset of $\mathbb{R}^n$.
(iii) The cone $C \in \mathcal{P}(\mathbb{R}^m)$ is closed, convex, pointed, and solid; let $e \in \text{int}(C)$ be a given element.
(iv) We assume that the vector-valued functions $F(\cdot,\zeta_1)$, $F(\cdot,\zeta_2)$, …, $F(\cdot,\zeta_p) : \mathbb{R}^n \to \mathbb{R}^m$ are twice continuously differentiable and locally strong convex.

We use the notation $F_\Omega(x)$ to denote the set $\{F(x,\zeta) : \zeta \in \Omega\}$. Note that, for a given $\mathscr{P}(\Omega)$, $F_\Omega : U \rightrightarrows \mathbb{R}^m$ is a set-valued function.

Definition 2.2. (Robust efficiency for UMOPs [6]). For a given UMOP $\mathscr{P}(\Omega)$, we call a feasible solution $\bar{x} \in U$

(i) robust efficient if there is no $x \in U \setminus \{\bar{x}\}$ such that set $F_\Omega(x) \subseteq F_\Omega(\bar{x}) - C$, and
(ii) weakly robust efficient if there is no $x \in U \setminus \{\bar{x}\}$ such that $F_\Omega(x) \subseteq F_\Omega(\bar{x}) - \text{int}(C)$.

In the next subsection, we give some basic properties of set optimization, and also define and interrelate robust efficient points of $\mathscr{P}(\Omega)$ and efficient points of a set-valued optimization problem with objective function F_Ω.

2.1. **Basics for set optimization and UMOPs.** In this section, we introduce the main notations used in the paper. The class of all nonempty subsets of $\mathbb{R}^m$ is denoted by $\mathcal{P}(\mathbb{R}^m)$. Furthermore, all the considered vectors are the column vectors, and we denote the transpose operator with the symbol $\top$. The notation $\|\cdot\|$ stands for either the Euclidean norm of a vector or for the standard spectral norm of a matrix, depending on the context. We also denote the cardinality of a finite set by $|A|$. For any $p \in \mathbb{N}$, we denote $[p] = \{1,2,\dots,p\}$.

Let C be a closed, convex, and pointed cone. Then, it generates a partial order $\preceq$ on $\mathbb{R}^m$ (see [24, 25]), as follows: $y \preceq z \iff z - y \in C$. Furthermore, if C is a solid cone, one can also find the strict order $\prec$, which is defined by $y \prec z \iff z - y \in \text{int}(C)$. Also, C^* denotes the polar cone of C.

In the following definition, we collect the concepts of maximal and weakly maximal elements of a set with respect to $\preceq$.

Definition 2.3. (i) The set of maximal elements of A with respect to C is defined as

$$\text{Max}(A,C) = \{y \in A : (y+C) \cap A = \{y\}\}.$$

(ii) The set of weakly maximal elements of A with respect to C is defined as

$$\text{WMax}(A,C) = \{y \in A : (y + \text{int}(C)) \cap A = \emptyset\}.$$

The proof of the following proposition is trivial, we omit the proof here.

Proposition 2.1. *Let $A \in \mathcal{P}(\mathbb{R}^m)$ be compact, and C be closed, convex, and pointed cone. Then, A satisfies the so-called domination property with respect to C, that is,* $A - C = \text{Max}(A,C) - C$.

The Gerstewitz scalarizing function also plays an important role in the main results.

Definition 2.4. Let C be closed, convex, pointed, and solid cone. For a given element $e \in \text{int}(C)$, the Gerstewitz functional associated with e and C is $\psi_e : \mathbb{R}^m \to \mathbb{R}$ defined by

$$\psi_e(y) = \min\{t \in \mathbb{R} : te \in y + C\}. \tag{2.3}$$

The useful properties of this function are summarized in the next proposition.

Proposition 2.2. [26]

(i) ψ_e *is sublinear and Lipschitz on* $\mathbb{R}^m$.

(ii) ψ_e *is both monotone and strictly monotone with respect to the partial order* $\preceq$, *i.e.,*

$$\forall\, y,z \in \mathbb{R}^m : y \preceq z \implies \psi_e(y) \leq \psi_e(z)$$
$$\textit{and}\ \forall\, y,z \in \mathbb{R}^m : y \prec z \implies \psi_e(y) < \psi_e(z),$$

respectively.

(iii) ψ_e *satisfies the representability property, i.e.,*

$$-C = \{y \in \mathbb{R}^m \,:\, \psi_e(y) \leq 0\}\ \textit{and}\ -\operatorname{int}(C) = \{y \in \mathbb{R}^m : \psi_e(y) < 0\}.$$

Definition 2.5. [27] For the given cone C, the upper set less relation $\preceq^u$ is the binary relation defined on $P(\mathbb{R}^m)$ as follows, for all $A,B \in P(\mathbb{R}^m)$,$A \preceq^u B \iff A \subseteq B - C$. Similarly, the strict upper set less relation $\prec^u$ is the binary relation defined on $P(\mathbb{R}^m)$ by, for all $A,B \in P(\mathbb{R}^m)$, $A \prec^u B \iff A \subseteq B - \operatorname{int}(C)$.

Suppose that $F_\Omega : \mathbb{R}^n \rightrightarrows \mathbb{R}^m$ is the set-valued mapping given by $F_\Omega(x) = \{F(x,\zeta) : \zeta \in \Omega\}$. Then, with upper set order relation on F_Ω, the given UMOP $\mathscr{P}(\Omega)$ can be viewed as a (deterministic) set-valued optimization problem

$$(\text{SOP}) \begin{cases} \min & F_\Omega(x) \\ \text{subject to} & x \in \mathbb{R}^n. \end{cases} \tag{2.4}$$

Note that a point $\bar{x} \in \mathbb{R}^n$ is a local weakly efficient solution of (SOP) if there exists a neighbourhood U of $\bar{x}$ such that the following holds:

$$\nexists x \in U : F_\Omega(x) \prec^u F_\Omega(\bar{x}),\ \text{i.e.,}\ \nexists x \in U : F_\Omega(x) \subseteq F_\Omega(\bar{x}) - \operatorname{int}(C).$$

From Definition 2.2, we see that a (weakly) efficient solution of (SOP) is a (weakly) robust efficient solution of the problem $\mathscr{P}(\Omega)$ and vice-versa. Thus, to identify robust weakly efficient points of the problem $\mathscr{P}(\Omega)$, one can aim to figure out weakly efficient solutions of the set optimization problem (SOP). In this paper, to find weakly efficient solutions of (SOP), we derive a Newton method.

3. Optimality Conditions for SOPs

In this section, we study optimality conditions for weakly efficient solutions of (SOP). These conditions are the foundation on which the proposed algorithm is built.

Definition 3.1. (i) The active index of maximal elements associated with the set-valued function F_Ω is $\mathscr{A} : \mathbb{R}^n \rightrightarrows [p]$, given by $\mathscr{A}(x) = \{i \in [p] : F(x,\zeta_i) \in \operatorname{Max}(F_\Omega(x),C)\}$.

(ii) The active index of weakly maximal elements associated with the set-valued function F_Ω is $\mathscr{A}_W : \mathbb{R}^n \rightrightarrows [p]$ defined as $\mathscr{A}_W(x) = \{i \in [p] : F(x,\zeta_i) \in \operatorname{WMax}\,(F_\Omega(x),C)\}$.

(iii) For a vector $\vartheta \in \mathbb{R}^m$, we define $\mathscr{A}_\vartheta : \mathbb{R}^n \rightrightarrows [p]$ as $\mathscr{A}_\vartheta(x) = \{i \in \mathscr{A}(x) : F(x,\zeta_i) = \vartheta\}$.

It follows from the definition that $\mathscr{A}_\vartheta(x) = \emptyset$ whenever $\vartheta \notin \operatorname{Max}(F_\Omega(x),C)$ and that

$$\mathscr{A}(x) = \bigcup_{\vartheta \in \operatorname{Max}(F_\Omega(x),C)} \mathscr{A}_\vartheta(x).$$

Definition 3.2. The map $\eta : \mathbb{R}^n \to \mathbb{R}$ is defined as the cardinality of the set of maximal elements of F_Ω, i.e., $\eta(x) = |\operatorname{Max}(F_\Omega(x),C)|$. Furthermore, we set $\bar{\eta} = \eta(\bar{x})$.

Definition 3.3. Let $x \in \mathbb{R}^n$, and $\{\vartheta_1^x, \vartheta_2^x, \ldots, \vartheta_{\eta(x)}^x\}$ be an enumeration of the set $\text{Max}(F_\Omega(x), C)$. The partition set at x is defined as $\mathscr{P}_x = \prod_{j=1}^{\eta(x)} \mathscr{A}_{\vartheta_j^x}(x)$, where $\mathscr{A}_{\vartheta_j^x}(x)$ is given in Definition 3.1 (iii).

The optimality conditions for UMOPs that we introduce are based on the following lemma. From the specific structure of the function F_Ω, we formulate a set of vector optimization problems. Subsequently, we apply optimality conditions to this collection of vector optimization problems to find weakly efficient points of the UMOP $\mathscr{P}(\Omega)$. The following lemma is the key step in this direction.

Lemma 3.1. *Let $\tilde{C} \in \mathcal{P}(\mathbb{R}^{m\bar{\eta}})$ be the cone $\tilde{C} = \prod_{j=1}^{\bar{\eta}} C$, and let $\preceq_{\tilde{C}}^u$ and $\prec_{\tilde{C}}^u$ denote the partial order and the strict order in $\mathbb{R}^{m\bar{\eta}}$ induced by $\tilde{C}$, respectively. Furthermore, consider the partition set $\mathscr{P}_{\bar{x}}$ at $\bar{x}$ and define, for every $\alpha = (\alpha_1, \alpha_2, \ldots, \alpha_{\bar{\eta}}) \in \mathscr{P}_{\bar{x}}$, the function $\tilde{F}(\cdot, \zeta_\alpha) : \mathbb{R}^n \times \Omega \to \prod_{j=1}^{\bar{\eta}} \mathbb{R}^m$ as $\tilde{F}(x, \zeta_\alpha) = \left(F(x, \zeta_{\alpha_1}), F(x, \zeta_{\alpha_2}), \ldots, F(x, \zeta_{\alpha_{\bar{\eta}}})\right)^\top$. Then, $\bar{x}$ is a local weakly robust efficient solution to (SOP) if and only if, for every $\alpha \in \mathscr{P}_{\bar{x}}$, $\bar{x}$ is a local weakly efficient solution to the vector optimization problem*

$$(VOP)(\zeta_\alpha) \begin{cases} \min & \tilde{F}(x, \zeta_\alpha), \\ \textit{subject to} & x \in \mathbb{R}^n. \end{cases} \tag{3.1}$$

Proof. We argue by the method of contradiction in both ways. First, assume that $\bar{x}$ is a local weakly robust efficient solution for (SOP) and that, for some $\alpha \in \mathscr{P}_{\bar{x}}$, $\bar{x}$ is not a local weakly efficient solution of $(VOP)(\zeta_\alpha)$. Then, we obtain a sequence $\{x_k\} \subseteq \mathbb{R}^n$ such that $x_k \to \bar{x}$ and

$$\{\tilde{F}(x_k, \zeta_\alpha)\} \subseteq \tilde{F}(\bar{x}, \zeta_\alpha) - \text{int}(\tilde{C}) \text{ for all } k \in \mathbb{N}. \tag{3.2}$$

From Proposition 2.1, we have

$$\begin{aligned} F_\Omega(x_k) &\subseteq \{F(x_k, \zeta_{\alpha_1}), F(x_k, \zeta_{\alpha_2}), \ldots, F(x_k, \zeta_{\alpha_{\bar{\eta}}})\} - C \text{ for all } k \in \mathbb{N} \\ &\subseteq \{F(\bar{x}, \zeta_{\alpha_1}), F(\bar{x}, \zeta_{\alpha_2}), \ldots, F(\bar{x}, \zeta_{\alpha_{\bar{\eta}}})\} - \text{int}(C) - C, \text{ using (3.2)} \\ &\subseteq F_\Omega(\bar{x}) - \text{int}(C) \text{ for all } k \in \mathbb{N}. \end{aligned}$$

Since $x_k \to \bar{x}$, as $k \to \infty$, this contradicts the weak robust efficiency of $\bar{x}$ for (SOP).

Next, suppose that $\bar{x}$ is a local weakly efficient solution of $(VOP)(\zeta_\alpha)$ for every $\alpha \in \mathscr{P}_{\bar{x}}$ but not a local weakly robust efficient solution of (SOP). Then, we obtain a sequence $\{x_k\} \subseteq \mathbb{R}^n$ such that $x_k \to \bar{x}$ and $F_\Omega(x_k) \subseteq F_\Omega(\bar{x}) - C$ for all $k \in \mathbb{N}$. Consider an enumeration $\{\vartheta_1^{\bar{x}}, \vartheta_2^{\bar{x}}, \ldots, \vartheta_{\bar{\eta}}^{\bar{x}}\}$ of the set $\text{Max}(F_\Omega(\bar{x}), C)$. Then,

$$\text{for all } j \in [\bar{\eta}], k \in \mathbb{N}, \exists\, i_{(j,k)} \in [p] \text{ such that } \{F(x_k, \zeta_{i_{(j,k)}})\} \subseteq \vartheta_j^{\bar{x}} - C. \tag{3.3}$$

Since the indexes $i_{(j,k)}$ are chosen on the finite set $[p]$, we can assume without loss of generality that $i_{(j,k)}$ is indendent of k, that is, $i_{(j,k)} = \bar{i}_j$ for every $k \in \mathbb{N}$ and some $\bar{i}_j \in [p]$. Hence, taking the limit in (3.3) when $k \to \infty$, we have

$$\text{for all } j \in [\bar{\eta}] : \{F(\bar{x}, \zeta_{\bar{i}_j})\} \subseteq \vartheta_j^{\bar{x}} - C. \tag{3.4}$$

Because $\vartheta_j^{\bar{x}} \in \text{Max}(F_\Omega(\bar{x}), C)$, it follows from (3.4) that $F(\bar{x}, \zeta_{\bar{i}_j}) = \vartheta_j^{\bar{x}}$ and that $\bar{i}_j \in \mathscr{A}(\bar{x})$ for every $j \in [\bar{\eta}]$. Consider now the tuple $\bar{\alpha} = (\bar{i}_1, \bar{i}_2, \ldots, \bar{i}_{\bar{\eta}})$. Then, it can be verified that $\bar{\alpha} \in \mathscr{P}_{\bar{x}}$. Also, from (3.2) we deduce that $\{\tilde{F}(x_k, \zeta_{\bar{\alpha}})\} \subseteq \tilde{F}(\bar{x}, \zeta_{\bar{\alpha}}) - \text{int}(\tilde{C})$ for every $k \in \mathbb{N}$. Since $x_k \to \bar{x}$, this contradics the weak efficiency of $\bar{x}$ for $(VOP)(\zeta_\alpha)$ when $\alpha = \bar{\alpha}$. ☐

We now establish the necessary optimality condition for UMOPs used in the Newton method. Since the proof is similar to [22, Theorem 3.1], we omit the proof here.

Theorem 3.1. *Suppose that $\bar{x}$ is a local weakly robust efficient solution for the UMOP $\mathscr{P}(\Omega)$. Then,*

$$\text{for all } \alpha \in \mathscr{P}_{\bar{x}},\ \exists\ \gamma_1, \gamma_2, \ldots, \gamma_{\bar{\eta}} \in C^* : \sum_{j=1}^{\bar{\eta}} \nabla F(\bar{x}, \zeta_{\alpha_j})\gamma_j = 0,\ (\gamma_1, \gamma_2, \ldots, \gamma_{\bar{\eta}}) \neq 0. \tag{3.5}$$

Conversely, assume that $F(\cdot, \zeta_i)$ is C-convex for each $i \in \mathscr{A}(\bar{x})$, i.e.,

$$\text{for all } i \in \mathscr{A}(\bar{x}),\ x_1, x_2 \in \mathbb{R}^n,\ t \in [0,1] : F(tx_1 + (1-t)x_2, \zeta_i) \preceq tF(x_1, \zeta_i) + (1-t)F(x_2, \zeta_i).$$

Then, condition (3.5) is also sufficient for a local weakly robust efficient point $\bar{x}$.

Definition 3.4. [22] We say that $\bar{x}$ is a stationary point for UMOP $\mathscr{P}(\Omega)$ if there exists a nonempty set $\mathscr{Q} \subseteq \mathscr{P}_{\bar{x}}$ such that

$$\text{for all } \alpha \in \mathscr{Q},\ \exists\ \gamma_1, \gamma_2, \ldots, \gamma_{\bar{\eta}} \in C^* : \sum_{j=1}^{\bar{\eta}} \nabla F(\bar{x}, \zeta_{\alpha_j})\gamma_j = 0,\ (\gamma_1, \gamma_2, \ldots, \gamma_{\bar{\eta}}) \neq 0. \tag{3.6}$$

If, in addition, we can choose $\mathscr{Q} = \mathscr{P}_{\bar{x}}$, we simply call $\bar{x}$ a strongly stationary point.

Since the proof is the following proposition is similar to [22, Proposition 3.1], we omit the proof here.

Proposition 3.1. *Let $\mathscr{Q} \subseteq \mathscr{P}_{\bar{x}}$ be given. Then, $\bar{x}$ is stationary for (SOP) with respect to $\mathscr{Q}$ if and only if*

$$\text{for all } \alpha \in \mathscr{Q}, d \in \mathbb{R}^n,\ \text{there exists } j \in [\bar{\eta}] \text{ such that } \nabla F(\bar{x}, \zeta_{\alpha_j})^\top d \notin -int(C).$$

Note that if $\bar{x}$ is a non-stationary point, then, for all $j \in [\bar{\eta}]$, there exist $\alpha \in \mathscr{P}_{\bar{x}}$ and $d \in \mathbb{R}^n$ such that

$$\begin{aligned} &\nabla F(\bar{x}, \zeta_{\alpha_j})^\top d \in -\text{int}(C), \\ \text{i.e., }\ &\psi_e(\nabla F(\bar{x}, \zeta_{\alpha_j})^\top d) < 0. \end{aligned} \tag{3.7}$$

Definition 3.5. [22] We say that $\bar{x}$ is a regular point of F_Ω in (SOP) if the following conditions are satisfied:

(i) $\text{Max}(F_\Omega(\bar{x}), C) = \text{WMax}(F_\Omega(\bar{x}), C)$ and
(ii) the cardinality function η, introduced in Definition 3.2, is constant in a neighborhood of $\bar{x}$.

4. Newton Method and Its Convergence Analysis

In this section, we present the solution approach. It is clearly based on the result shown in Lemma 3.1. At every iteration, an element α in the partition set of the current iterate is selected, and then, a descent direction for $(VOP)(\zeta_\alpha)$ will be found using ideas from [28, 29]. However, one must be careful with the selection process of the element α to guarantee convergence. Thus, we propose a specific way to achieve this. After determining the descent direction, we follow a classical backtracking procedure of Armijo type to determine a suitable step size and update the iterate in the desired direction.

Algorithm 1 Newton Method to Solve $\mathscr{P}(\Omega)$

Step 0: Choose $x_0 \in \mathbb{R}^n,\ \rho \in (0,1)$. Set $k = 0$ and define $\mathcal{N} = \{\frac{1}{2^n} : n = 0,1,2,\ldots\}$.
Step 1: Compute

$$\mathscr{R}_k = \mathrm{Max}(F_\Omega(x_k),C),\ \mathscr{P}_k = \mathscr{P}_{x_k},\ \eta_k = |\mathrm{Max}(F_\Omega(x_k),C)|.$$

Step 2: Find

$$(\alpha_k,d_k) \in \underset{(\alpha,d)\in\mathscr{P}_k\times\mathbb{R}^n}{\mathrm{argmin}}\ \max_{j\in[\eta_k]}\left\{\psi_e\left(\nabla F(x_k,\zeta_{\alpha_j})^\top d + \tfrac{1}{2}d^\top\nabla^2 F(x_k,\zeta_{\alpha_j})d\right)\right\}$$

Step 3: If $d_k = 0$, stop. Otherwise, go to Step 4.
Step 4: Choose τ_k as the largest $\tau \in \mathcal{N}$ such that

$$F(x_k+\tau d_k,\zeta_{\alpha_{k,j}}) \preceq F(x_k,\zeta_{\alpha_{k,j}}) + \rho\tau\left(\nabla F(x_k,\zeta_{\alpha_{k,j}})^\top d_k + \tfrac{1}{2}d_k^\top\nabla^2 F(x_k,\zeta_{\alpha_{k,j}})d_k\right)\ \text{ for all } j \in [\eta_k].$$

Step 5: Set $x_{k+1} = x_k + \tau_k d_k,\ k = k+1$ and go to Step 2.

For the rest of the analysis, we need to introduce the parametric family of functions $\{\mathscr{G}_x\}_{x\in\mathbb{R}^n}$, whose elements $\mathscr{G}_x : \mathscr{P}_x \times \mathbb{R}^n \to \mathbb{R}$ are defined as follows:

$$\text{for all } \alpha \in \mathscr{P}_x,\ d \in \mathbb{R}^n:\ \mathscr{G}_x(\alpha,d) = \max_{j\in[\eta(x)]}\left\{\psi_e\left(\nabla F(x,\zeta_{\alpha_j})^\top d + \tfrac{1}{2}d^\top\nabla^2 F(x,\zeta_{\alpha_j})d\right)\right\}, \tag{4.1}$$

where the functional ψ_e is given by (2.3). It is easy to see from assumption (iv) that, for every $x \in \mathbb{R}^n$ and $\alpha \in \mathscr{P}_x$, the functional $\mathscr{G}_x(\alpha,\cdot)$ is strongly convex in $\mathbb{R}^n$, i.e., there exists a constant $\beta > 0$ such that the inequality

$$\mathscr{G}_x(\alpha,td+(1-t)d') + \beta t(1-t)\|d-d'\|^2 \le t\mathscr{G}_x(\alpha,d) + (1-t)\mathscr{G}_x(\alpha,d')$$

is satisfied for every $d,d' \in \mathbb{R}^n$ and $t \in [0,1]$. According to [30], $\mathscr{G}_x(\alpha,\cdot)$ attains its minimum over $\mathbb{R}^n$, and this minimum is unique.

Taking into account that $\mathscr{P}_x$ is finite, we also obtain that $\mathscr{G}_x$ attains its minimum over the set $\mathscr{P}_x \times \mathbb{R}^n$. Hence we can consider the function $\mathcal{G} : \mathbb{R}^n \to \mathbb{R}$ given by

$$\mathcal{G}(x) = \min_{(\alpha,d)\in\mathscr{P}_x\times\mathbb{R}^n} \mathscr{G}_x(\alpha,d). \tag{4.2}$$

Now, we examine several properties of the function $\mathcal{G}$ and investigate its connection with the descent direction d and the stationarity of the point x.

Proposition 4.1. *Consider the functions $\mathscr{G}_{\bar{x}}$ and $\mathcal{G}$ given in (4.1) and (4.2), respectively. Furthermore, let $(\bar{\alpha},\bar{d}) \in \mathscr{P}_{\bar{x}} \times \mathbb{R}^n$ be such that $\mathcal{G}(\bar{x}) = \mathscr{G}_{\bar{x}}(\bar{\alpha},\bar{d})$. Then, the following statements are equivalent:*

(i) *$\bar{x}$ is not a stationary point of UMOP $\mathscr{P}(\Omega)$.*
(ii) $\mathcal{G}(\bar{x}) < 0$.
(iii) $\bar{d} \neq 0$.

Proof. *(i)* $\implies$ *(ii)* Let us assume that $\bar{x}$ is a non-stationary point of UMOP. Then, for all $j \in [\bar{\eta}]$, there exists an $\alpha = (\alpha_1,\alpha_2,\ldots,\alpha_{\bar{\eta}}) \in \mathscr{P}_{\bar{x}}$ and $\bar{d} \in \mathbb{R}^n$ with $\nabla F(\bar{x},\zeta_{\alpha_j})^\top\bar{d} \in -\mathrm{int}(C)$, i.e., $\psi_e(\nabla F(\bar{x},\zeta_{\alpha_j})^\top \bar{d}) < 0$. Now, we note that

$$\begin{aligned} \mathcal{G}(\bar{x}) &\leq \min_{(\alpha,d)\in\mathscr{P}_{\bar{x}}\times\mathbb{R}^n} \mathscr{G}_{\bar{x}}(\alpha,d) \\ &\leq \mathscr{G}_{\bar{x}}(\alpha,t\bar{d}), \quad \text{for some } t>0 \\ &= t \max_{j\in[\eta(\bar{x})]} \left\{ \psi_e\left(\nabla F(\bar{x},\zeta_{\alpha_j})^\top \bar{d} + \tfrac{t}{2}\bar{d}^\top \nabla^2 F(\bar{x},\zeta_{\alpha_j})\bar{d}\right) \right\}. \end{aligned}$$

Therefore, for $t>0$, small enough, from assumption (iv), the right-hand side of the above inequality is negative. Thus (ii) holds.

$(ii) \implies (iii)$ Note that $\mathcal{G}(\bar{x})$ is optimal value of $\mathscr{G}_{\bar{x}}(\alpha,d)$, given in (4.1), and $\mathscr{G}_{\bar{x}}(\alpha,0)=0$ for any α in $\mathscr{P}_{\bar{x}}$. As $\mathcal{G}(\bar{x})$ is negative, $\bar{d}\neq 0$.

$(iii) \implies (i)$ Let us assume that $\bar{x}$ is a stationary point. Then, for any $\alpha\in\mathscr{P}_{\bar{x}}$ and $d\in\mathbb{R}^n$, there exists $j\in[\bar{\eta}]$ such that $\nabla F(\bar{x},\zeta_{\alpha_j})^\top d \notin -\text{int}(C)$, i.e., $\psi_e(\nabla F(\bar{x},\zeta_{\alpha_j})^\top d)\geq 0$. Also, since, for all $j\in[\eta(\bar{x})]$, $\nabla^2 F(\bar{x},\zeta_{\alpha_j})$'s are positive definite matrices, i.e., for any $d\in\mathbb{R}^n$, $d^\top \nabla^2 F(\bar{x},\zeta_{\alpha_j})d>0$, we obtain

$$\begin{aligned} 0 &\leq \psi_e(\nabla F(\bar{x},\zeta_{\alpha_j})^\top d) \\ &< \psi_e\left(\nabla F(\bar{x},\zeta_{\alpha_j})^\top d + \tfrac{1}{2}d^\top \nabla^2 F(\bar{x},\zeta_{\alpha_j})d\right) \\ &\leq \max_{j\in[\eta(\bar{x})]} \left\{ \psi_e\left(\nabla F(\bar{x},\zeta_{\alpha_j})^\top d + \tfrac{1}{2}d^\top \nabla^2 F(\bar{x},\zeta_{\alpha_j})d\right) \right\} \\ &= \mathscr{G}_{\bar{x}}(\alpha,d) \text{ using (4.1)}, \end{aligned}$$

$$\text{i.e., } 0\leq \mathscr{G}_{\bar{x}}(\alpha,d) \leq \min_{(\alpha,d)\in\mathscr{P}_{\bar{x}}\times\mathbb{R}^n} \mathscr{G}_{\bar{x}}(\alpha,d), \text{i.e., } 0\leq \mathcal{G}(\bar{x}) < 0 \text{ by using (4.2)}.$$

This is a contradiction, so $\bar{x}$ is a non-stationary point for the UMOP. □

Theorem 4.1. *Let U be a nonempty open subset of $\mathbb{R}^n$. The function $\mathcal{G}: U\to\mathbb{R}$, defined in (4.2), is continuous.*

Proof. Let $\{x_k\}$ be a sequence which converges to $\bar{x}\in\mathbb{R}^n$. We show that $\lim_{k\to\infty}\mathcal{G}(x_k)=\mathcal{G}(\bar{x})$. From the definition of $\mathcal{G}$ at $\bar{x}$, we have

$$\begin{aligned} \mathcal{G}(\bar{x}) &\leq \mathscr{G}_{\bar{x}}(\alpha_k,d_k) \\ &= \max_{j\in[\eta(x)]} \psi_e\left(\nabla F(\bar{x},\zeta_{\alpha_j})^\top d_k + \tfrac{1}{2}d_k^\top \nabla^2 F(\bar{x},\zeta_{\alpha_j})d_k\right) \\ &= \max_{j\in[\eta(x)]} \psi_e\Big(\nabla F(\bar{x},\zeta_{\alpha_j})^\top d_k + \tfrac{1}{2}d_k^\top \nabla^2 F(\bar{x},\zeta_{\alpha_j})d_k - \nabla F(x_k,\zeta_{\alpha_j})^\top d_k - \tfrac{1}{2}d_k^\top \nabla^2 F(x_k,\zeta_{\alpha_j})d_k \\ &\quad + \nabla F(x_k,\zeta_{\alpha_j})^\top d_k + \tfrac{1}{2}d_k^\top \nabla^2 F(x_k,\zeta_{\alpha_j})d_k\Big) \\ &\leq \max_{j\in[\eta(x)]} \psi_e\left(\nabla F(x_k,\zeta_{\alpha_j})^\top d_k + \tfrac{1}{2}d_k^\top \nabla^2 F(x_k,\zeta_{\alpha_j})d_k\right) + \max_{j\in[\eta(x)]} \psi_e\Big(\nabla F(\bar{x},\zeta_{\alpha_j})^\top d_k \\ &\quad + \tfrac{1}{2}d_k^\top \nabla^2 F(\bar{x},\zeta_{\alpha_j})d_k - \nabla F(x_k,\zeta_{\alpha_j})^\top d_k - \tfrac{1}{2}d_k^\top \nabla^2 F(x_k,\zeta_{\alpha_j})d_k\Big). \end{aligned}$$

Using properties of the Grestewitz functional ψ_e, given in Proposition 2.2 (i), with a Lipschitz constant L, we have

$$\begin{aligned} \mathcal{G}(\bar{x}) &= \mathscr{G}_{x_k}(\alpha_k,d_k) \\ &\quad + L \max_{j\in[\eta(x)]} \|\nabla F(\bar{x},\zeta_{\alpha_j})^\top d_k + \tfrac{1}{2}d_k^\top \nabla^2 F(\bar{x},\zeta_{\alpha_j})d_k - \nabla F(x_k,\zeta_{\alpha_j})^\top d_k - \tfrac{1}{2}d_k^\top \nabla^2 F(x_k,\zeta_{\alpha_j})d_k\| \end{aligned}$$

$$\leq \mathscr{G}_{x_k}(\alpha_k, d_k) + L \max_{j\in[\eta(x)]} \|\nabla F(\bar{x}, \zeta_{\alpha_j})^\top d_k - \nabla F(x_k, \zeta_{\alpha_j})^\top d_k\|$$
$$+ \frac{L}{2} \max_{j\in[\eta(x)]} \|d_k^\top \nabla^2 F(\bar{x}, \zeta_{\alpha_j}) d_k - d_k^\top \nabla^2 F(x_k, \zeta_{\alpha_j}) d_k\|$$
$$\leq \mathscr{G}_{x_k}(\alpha_k, d_k) + L \max_{j\in[\eta(x)]} \|\nabla F(\bar{x}, \zeta_{\alpha_j}) - \nabla F(x_k, \zeta_{\alpha_j})\| \|d_k\|$$
$$+ \frac{L}{2} \max_{j\in[\eta(x)]} \|\nabla^2 F(\bar{x}, \zeta_{\alpha_j}) - \nabla^2 F(x_k, \zeta_{\alpha_j})\| \|d_k\|^2.$$

Taking $k \to \infty$, we have

$$\mathcal{G}(\bar{x}) \leq \lim_{k\to\infty} \mathscr{G}(x_k). \tag{4.3}$$

For any $k \in \mathbb{N}$, we have $\mathcal{G}(x_k) = \min_{(\alpha_k, d_k)\in \mathscr{P}_{x_k}\times\mathbb{R}^n} \mathscr{G}_{x_k}(\alpha_k, d_k) \leq \mathscr{G}_{x_k}(\alpha_k, d_k)$. Since the function $\mathscr{G}_{x_k}$ is continuous, we obtain

$$\lim_{k\to\infty} \mathcal{G}(x_k) \leq \lim_{k\to\infty} \mathscr{G}_{x_k}(\alpha_k, d_k) = \mathscr{G}_{\bar{x}}(\bar{\alpha}, \bar{d}) = \min_{(\alpha,d)\in\mathscr{P}_{\bar{x}}\times\mathbb{R}^n} \mathscr{G}_{\bar{x}}(\alpha, d) = \mathcal{G}(\bar{x}).$$

We can obtain the required result by combining the last inequality and (4.3). □

The fundamental characteristic of the Newton method in scalar minimization and equation-solving is its utilization of quadratic and linear approximations, respectively. In the following lemma, we estimate the errors incurred when approximating $F(\cdot, \zeta)$ and $\nabla F(\cdot, \zeta)$by using their quadratic and linear models, respectively.

Lemma 4.1. [22, 29] *Suppose that $\bar{x}$ is a regular point of F_Ω.*

(i) *Then, there exists a neighborhood U of $\bar{x}$ such that, for every $x \in U$, $\eta(x) = \eta(\bar{x})$.*

(ii) *Let $\varepsilon > 0$ and $\delta > 0$ be such that, for any $x, y \in U$, with $\|y - x\| < \delta$,*

$$\|\nabla^2 F(y, \zeta_{\alpha_j}) - \nabla^2 F(x, \zeta_{\alpha_j})\| < \varepsilon \text{ for all } j = 1, 2, \ldots, [\eta(\bar{x})].$$

Under this assumption, for any $x, y \in U$ such that $\|y - x\| < \delta$, we have that

(a)

$$\|\nabla F(y, \zeta_{\alpha_j}) - [\nabla F(x, \zeta_{\alpha_j}) + \nabla^2 F(x, \zeta_{\alpha_j})(y - x)]\| < \varepsilon \|y - x\|$$

and

(b)

$$\|F(y, \zeta_{\alpha_j}) - [F(x, \zeta_{\alpha_j}) + \nabla F(x, \zeta_{\alpha_j})^\top (y - x) + \tfrac{1}{2}(y - x)^\top \nabla^2 F(x, \zeta_{\alpha_j})(y - x)]\| < \tfrac{\varepsilon}{2}\|y - x\|^2$$

for all $j = 1, 2, \ldots, [\eta(\bar{x})]$.

(c) *If $\nabla^2 F(\cdot, \zeta_{\alpha_j})$ is Lipschitz continuous on U with constant L for $j = 1, 2, \ldots, [\eta(\bar{x})]$, then*

$$\|\nabla F(y, \zeta_{\alpha_j}) - [\nabla F(x, \zeta_{\alpha_j}) + \nabla^2 F(x, \zeta_{\alpha_j})(y - x)]\| < \tfrac{L}{2}\|y - x\|^2 \text{ for all } j = 1, 2, \ldots, [\eta(\bar{x})].$$

In the next theorem, we aim to prove that the iterative process involved in the line search of the fourth step in Algorithm 1 terminates within a finite number of steps.

Theorem 4.2. *Fix $\rho \in (0, 1)$ and consider the functions $\mathscr{G}_{\bar{x}}$ and $\mathcal{G}$ given in (4.1) and (4.2), respectively. Furthermore, let $(\bar{\alpha}, \bar{d}) \in \mathscr{P}_{\bar{x}} \times \mathbb{R}^n$ be such that $\mathcal{G}(\bar{x}) = \mathscr{G}_{\bar{x}}(\bar{\alpha}, \bar{d})$ and suppose that $\bar{x}$ is not a stationary point of (SOP). Then, the following assertions hold.*

(i) *There exists* $\tilde{\tau} > 0$ *such that*

$$\text{for all } \tau \in (0, \tilde{\tau}], j \in [\bar{\eta}] : F(\bar{x} + \tau\bar{d}, \zeta_{\bar{\alpha}_j}) \preceq F(\bar{x}, \zeta_{\bar{\alpha}_j}) + \rho\tau\big(\nabla F(\bar{x}, \zeta_{\bar{\alpha}_j})^\top \bar{d} + \tfrac{1}{2}\bar{d}^\top \nabla^2 F(\bar{x}, \zeta_{\bar{\alpha}_j})\bar{d}\big). \tag{4.4}$$

(ii) *Let* $\tilde{\tau}$ *be the parameter in statement* (i). *Then,*

$$\text{for all } \tau \in (0, \tilde{\tau}] : F_\Omega(\bar{x} + \tau\bar{d}) \preceq^u \big\{F(\bar{x}, \zeta_{\bar{\alpha}_j}) + \rho\tau\big(\nabla F(\bar{x}, \zeta_{\bar{\alpha}_j})^\top \bar{d} + \tfrac{1}{2}\bar{d}^\top \nabla^2 F(\bar{x}, \zeta_{\bar{\alpha}_j})\bar{d}\big)\big\}_{j\in[\bar{\eta}]}$$
$$\prec^u F_\Omega(\bar{x}).$$

Proof. (i) Assume that (i) does not hold. Then, we could find a sequence $\{\tau_k\}_{k\geq 1}$ and $\bar{j} \in [\bar{\eta}]$ such that $\tau_k \to 0$ and, for all $k \in \mathbb{N}$,

$$F(\bar{x} + \tau_k\bar{d}, \zeta_{\bar{\alpha}_j}) \notin F(\bar{x}, \zeta_{\bar{\alpha}_j}) + \rho\tau_k\big(\nabla F(\bar{x}, \zeta_{\bar{\alpha}_j})^\top \bar{d} + \tfrac{1}{2}\bar{d}^\top \nabla^2 F(\bar{x}, \zeta_{\bar{\alpha}_j})\bar{d}\big) - C. \tag{4.5}$$

Multiply both sides by $\frac{1}{\tau_k}$ in (4.5) for each $k \in \mathbb{N}$ to obtain, for all $k \in \mathbb{N}$,

$$\frac{F(\bar{x} + \tau_k\bar{d}, \zeta_{\bar{\alpha}_j}) - F(\bar{x}, \zeta_{\bar{\alpha}_j})}{\tau_k} \notin \rho\big(\nabla F(\bar{x}, \zeta_{\bar{\alpha}_j})^\top \bar{d} + \tfrac{1}{2}\bar{d}^\top \nabla^2 F(\bar{x}, \zeta_{\bar{\alpha}_j})\bar{d}\big) - C.$$

Now, taking the limit $k \to \infty$ in the inequality above, we see

$$\nabla F(\bar{x}, \zeta_{\bar{\alpha}_j})^\top \bar{d} - \rho\big(\nabla F(\bar{x}, \zeta_{\bar{\alpha}_j})^\top \bar{d} + \tfrac{1}{2}\bar{d}^\top \nabla^2 F(\bar{x}, \zeta_{\bar{\alpha}_j})\bar{d}\big) \notin -\mathrm{int}(C). \tag{4.6}$$

Since $\bar{x}$ is not stationary point, we can apply Proposition 4.1 to obtain that $\bar{d} \neq 0$ and that $\mathcal{G}(\bar{x}) < 0$. Using the continuity of $\mathcal{G}$ (see Theorem 4.1), there exists $r > 0$ such that

$$\mathcal{G}(x) \leq \tfrac{1}{2}\mathcal{G}(\bar{x}) \text{ for all } x \in B[\bar{x}, r].$$

From [28, Lemma 3.2], d is bounded in $B[\bar{x}, r]$. We take a sequence of $\{d_k\}$ in $B[\bar{x}, r]$, which converges to $\bar{d}$. Now using Taylor's expansion, we have

$$F(x + \tau_k d_k, \zeta_{\alpha_j}) = F(x, \zeta_{\alpha_j}) + \tau_k \nabla F(x, \zeta_{\alpha_j})^\top d_k + o_j(\tau_k d_k, x)e \text{ for all } j \in [\eta(x)],$$

where $e = (1, 1, \ldots, 1)^\top$ and $\lim_{k\to\infty} \frac{o_j(\tau_k d_k, x)e}{\tau_k\|d_k\|} = (0, 0, \ldots, 0)^\top$. Since $\{d_k\}$ is bounded on $B[\bar{x}, r]$, one has

$$\lim_{k\to\infty} \frac{o_j(\tau_k d_k, x)e}{\tau_k} = (0, 0, \ldots, 0)^\top.$$

Observe that $\nabla F(x, \zeta_{\alpha_j})^\top d_k \preceq \nabla F(x, \zeta_{\alpha_j})^\top d + \frac{1}{2}d^\top \nabla^2 F(x, \zeta_{\alpha_j})d$. For all $j \in [\eta(x)]$, we conclude that

$$F(x + \tau_k d_k, \zeta_{\alpha_j}) \preceq F(x, \zeta_{\alpha_j}) + \tau_k\big(\nabla F(x, \zeta_{\alpha_j})^\top d + \tfrac{1}{2}d^\top \nabla^2 F(x, \zeta_{\alpha_j})d\big) + o_j(\tau_k d_k, x)e.$$

It follows that

$$\begin{aligned}&\frac{F(x + \tau_k d_k, \zeta_{\alpha_j}) - F(x, \zeta_{\alpha_j})}{\tau_k}\\ &\preceq \rho\big(\nabla F(x, \zeta_{\alpha_j})^\top d + \tfrac{1}{2}d^\top \nabla^2 F(x, \zeta_{\alpha_j})d\big)\\ &\quad + \tau_k\big[(1-\rho)\big(\nabla F(x, \zeta_{\alpha_j})^\top d_k + \tfrac{1}{2}d^\top \nabla^2 F(x, \zeta_{\alpha_j})d\big) + \tfrac{o_j(\tau_k d_k, x)e}{\tau_k}\big].\end{aligned}$$

Taking limit $k \to \infty$, we have

$$\begin{aligned} &\nabla F(x,\zeta_{\alpha_j})^\top d \prec \rho\big(\nabla F(x,\zeta_{\alpha_j})^\top d + \tfrac{1}{2} d^\top \nabla^2 F(x,\zeta_{\alpha_j}) d\big), \\ \text{i.e., } &\nabla F(x,\zeta_{\alpha_j})^\top d - \rho\big(\nabla F(x,\zeta_{\alpha_j})^\top d + \tfrac{1}{2} d^\top \nabla^2 F(x,\zeta_{\alpha_j}) d\big) \in -\mathrm{int}(C) \\ &\text{for all } x \in B[\bar{x},r] \text{ and } j \in [\eta(x)]. \end{aligned}$$

In particular, for $x = \bar{x}$, we have a contradiction to (4.6). Hence, statement (i) is proved.

(ii) Since $\bar{x}$ is not a stationary point, we see from Proposition 4.1 that

$$\begin{aligned} &\mathcal{G}(\bar{x}) < 0, \\ \text{i.e., } &\mathscr{G}_{\bar{x}}(\bar{\alpha},\bar{d}) < 0, \\ \text{i.e., } &\max_{j \in [\bar{\eta}]} \big\{ \psi_e\big(\nabla F(\bar{x},\zeta_{\bar{\alpha}_j})^\top \bar{d} + \tfrac{1}{2}\bar{d}^\top \nabla^2 F(\bar{x},\zeta_{\bar{\alpha}_j})\bar{d}\big)\big\} < 0, \\ \text{i.e., } &\text{ for any } j \in [\bar{\eta}],\ \psi_e\big(\nabla F(\bar{x},\zeta_{\bar{\alpha}_j})^\top \bar{d} + \tfrac{1}{2}\bar{d}^\top \nabla^2 F(\bar{x},\zeta_{\bar{\alpha}_j})\bar{d}\big) < 0, \\ \text{i.e., } &\nabla F(\bar{x},\zeta_{\bar{\alpha}_j})^\top \bar{d} + \tfrac{1}{2}\bar{d}^\top \nabla^2 F(\bar{x},\zeta_{\bar{\alpha}_j})\bar{d} \in -\mathrm{int}(C). \end{aligned}$$

Using this in inequality (4.4), we have

$$\begin{aligned} \text{for all } \tau \in (0,\tilde{\tau}], j \in [\bar{\eta}] : F(\bar{x}+\tau\bar{d},\zeta_{\bar{\alpha}_j}) & \\ &\preceq F(\bar{x},\zeta_{\bar{\alpha}_j}) + \rho\tau\big(\nabla F(\bar{x},\zeta_{\bar{\alpha}_j})^\top \bar{d} + \tfrac{1}{2}\bar{d}^\top \nabla^2 F(\bar{x},\zeta_{\bar{\alpha}_j})\bar{d}\big) \\ &\prec F(\bar{x},\zeta_{\bar{\alpha}_j}). \end{aligned}$$

Then, it follows that

$$\begin{aligned} F_\Omega(\bar{x}+\tau\bar{d}) &\subseteq \big\{F(\bar{x}+\tau\bar{d},\zeta_{\bar{\alpha}_j})\big\}_{j\in[\bar{\eta}]} - C \\ &\subseteq \big\{F(\bar{x},\zeta_{\bar{\alpha}_j}) + \rho\tau\big(\nabla F(\bar{x},\zeta_{\bar{\alpha}_j})^\top \bar{d} + \tfrac{1}{2}\bar{d}^\top \nabla^2 F(\bar{x},\zeta_{\bar{\alpha}_j})\bar{d}\big)\big\}_{j\in[\bar{\eta}]} - C \\ &\subseteq \big\{F(\bar{x},\zeta_{\bar{\alpha}_j})\big\}_{j\in[\bar{\eta}]} - \mathrm{int}(C) - C \\ &\subseteq \big\{F(\bar{x},\zeta_{\bar{\alpha}_1}), F(\bar{x},\zeta_{\bar{\alpha}_2}), \ldots, F(\bar{x},\zeta_{\bar{\alpha}_{\bar{\eta}}})\big\} - \mathrm{int}(C) \\ &\subseteq F_\Omega(\bar{x}) - \mathrm{int}(C). \end{aligned}$$

Hence, statement (ii) is proved.

□

In the following theorem, we give the convergence of the proposed method.

Theorem 4.3. *Suppose that* Algorithm 1 *generates an infinite sequence for which $\bar{x}$ is an accumulation point. Furthermore, assume that $\bar{x}$ is a regular point for F_Ω. Then, $\bar{x}$ is a stationary point of (SOP).*

Proof. Consider the function $\mu(A) = \sup_{y\in A} \psi_e(y)$. First, we show the following result

$$\text{for all } k \in \mathbb{N}\cup\{0\} : (\mu\circ F_\Omega)(x_{k+1}) \leq (\mu\circ F_\Omega)(x_k) + \rho\tau_k \mathscr{G}(x_k).$$

Indeed, because of the monotonicity property of ψ_e in Proposition 2.2 (ii), μ is monotone with respect to the preorder $\preceq^u$, that is, for all $A, B \in \mathscr{P}(\mathbb{R}^m)$, $A \preceq^u B \implies \mu(A) \leq \mu(B)$. For all

$k \in \mathbb{N} \cup \{0\}$,

$$F_\Omega(x_k + \tau_k d_k) \preceq \left\{ F(x_k, \zeta_{k,\alpha_j}) + \rho \tau_k \left(\nabla F(x_k, \zeta_{k,\alpha_j})^\top d_k + \tfrac{1}{2} d_k{}^\top \nabla^2 F(x_k, \zeta_{k,\alpha_j}) d_k \right) \right\}_{j \in [\eta_k]}.$$

Hence, using the monotonicity of μ and the sublinearity of ψ_e, we obtain for any $k \in \mathbb{N} \cup \{0\}$ that

$$\begin{aligned}
&(\mu \circ F_\Omega)(x^{k+1}) \\
&\le \max_{j \in [\eta_k]} \left\{ \psi_e\left(F(x_k, \zeta_{k,\alpha_j}) + \rho \tau_k \left(\nabla F(x_k, \zeta_{k,\alpha_j})^\top d_k + \tfrac{1}{2} d_k{}^\top \nabla^2 F(x_k, \zeta_{k,\alpha_j}) d_k \right) \right) \right\} \\
&\le \max_{j \in [\eta_k]} \left\{ \psi_e\left(F(x_k, \zeta_{k,\alpha_j}) \right) + \rho \tau_k \psi_e\left(\nabla F(x_k, \zeta_{k,\alpha_j})^\top d_k + \tfrac{1}{2} d_k{}^\top \nabla^2 F(x_k, \zeta_{k,\alpha_j}) d_k \right) \right\} \\
&\le \max_{j \in [\eta_k]} \psi_e\left(F(x_k, \zeta_{k,\alpha_j}) \right) + \rho \tau_k \max_{j \in [\eta_k]} \psi_e\left(\nabla F(x_k, \zeta_{k,\alpha_j})^\top d_k + \tfrac{1}{2} d_k{}^\top \nabla^2 F(x_k, \zeta_{k,\alpha_j}) d_k \right) \\
&= (\mu \circ F_\Omega)(x_k) + \rho \tau_k \max_{j \in [\eta_k]} \psi_e\left(\nabla F(x_k, \zeta_{k,\alpha_j})^\top d_k + \tfrac{1}{2} d_k{}^\top \nabla^2 F(x_k, \zeta_{k,\alpha_j}) d_k \right),
\end{aligned}$$

that is,

$$-\rho \tau_k \max_{j \in [\eta_k]} \psi_e\left(\nabla F(x_k, \zeta_{k,\alpha_j})^\top d_k + \tfrac{1}{2} d_k{}^\top \nabla^2 F(x_k, \zeta_{k,\alpha_j}) d_k \right) \le (\mu \circ F_\Omega)(x_k) - (\mu \circ F_\Omega)(x_{k+1}).$$

Adding the above inequality for $k = 0, 1, 2, \ldots, \bar{k}$, we have

$$-\rho \sum_{k=0}^{\bar{k}} \tau_k \max_{j \in [\eta_k]} \psi_e\left(\nabla F(x_k, \zeta_{k,\alpha_j})^\top d_k + \tfrac{1}{2} d_k{}^\top \nabla^2 F(x_k, \zeta_{k,\alpha_j}) d_k \right) \le (\mu \circ F_\Omega)(x_0) - (\mu \circ F_\Omega)(x_{k+1}).$$

On the other hand, we have

$$\nabla F(x_k, \zeta_{k,\alpha_j})^\top d_k + \tfrac{1}{2} d_k{}^\top \nabla^2 F(x_k, \zeta_{k,\alpha_j}) d_k \in -\operatorname{int}(C). \tag{4.7}$$

In particular, applying Proposition 2.2 in (4.7), we find for all $k \in \mathbb{N} \cup \{0\}, j \in [\eta_k]$ that

$$\psi_e\left(\nabla F(x_k, \zeta_{k,\alpha_j})^\top d_k + \tfrac{1}{2} d_k{}^\top \nabla^2 F(x_k, \zeta_{k,\alpha_j}) d_k \right) < 0.$$

We then have

$$\begin{aligned}
0 &< -\sum_{k=0}^{\bar{k}} \tau_k \max_{j \in [\eta_k]} \psi_e\left(\nabla F(x_k, \zeta_{k,\alpha_j})^\top d_k + \tfrac{1}{2} d_k{}^\top \nabla^2 F(x_k, \zeta_{k,\alpha_j}) d_k \right) \\
&\le \frac{(\mu \circ F_\Omega)(x_0) - (\mu \circ F_\Omega)(x_{k+1})}{\rho}.
\end{aligned}$$

Taking now the limit in the previous inequality when $k \to \infty$, we deduce that

$$0 \le -\sum_{k=0}^{\bar{k}} \tau_k \max_{j \in [\eta_k]} \psi_e\left(\nabla F(x_k, \zeta_{k,\alpha_j})^\top d_k + \tfrac{1}{2} d_k{}^\top \nabla^2 F(x_k, \zeta_{k,\alpha_j}) d_k \right) < \infty.$$

Therefore, in particular, this implies that

$$\lim_{k \to \infty} \tau_k \max_{j \in [\eta_k]} \psi_e\left(\nabla F(x_k, \zeta_{k,\alpha_j})^\top d_k + \tfrac{1}{2} d_k{}^\top \nabla^2 F(x_k, \zeta_{k,\alpha_j}) d_k \right) = 0,$$

$$\text{i.e., } \lim_{k \to \infty} \tau_k \mathscr{G}(x_k) = 0. \tag{4.8}$$

Since there are only a finite number of subsets of $[p]$ and $\bar{x}$ is regular for F_Ω, we can apply the Lemma 4.2 of [22], from which, without loss of generality, we see that there exist a subsequence $\mathscr{K}$ in $\mathbb{N}$, $\mathcal{Q} \subseteq \mathscr{P}_{\bar{x}}$ and $\bar{\alpha} \in \mathscr{Q}$ such that, for all $k \in \mathscr{K}$, $\eta_k = \bar{\eta}$, $\mathscr{P}_{x_k} = \mathscr{Q}$, $\alpha_k = \bar{\alpha}$. Furthermore, since the sequences $\{\tau_k\}$ and $\{d_k\}$ are bounded, there exist $\bar{\tau}$ and $\bar{d}$ such that $\tau_k \to \bar{\tau}$ and $d_k \to \bar{d}$. Suppose that $\bar{x}$ is nonstationary, which, by Proposition 4.1, is equivalent to $\mathscr{G}(\bar{x}) < 0$ and $\bar{d} \neq 0$. Using Theorem 4.2 (ii), we conclude that there exists an integer q such that

$$\mu \circ (F_\Omega(\bar{x} + 2^{-q}\bar{d}) - F_\Omega(\bar{x})) < \rho 2^{-q}\mathscr{G}(\bar{x}).$$

Since $\mathscr{G}$ and μ are continuous in their respective domains,

$$\lim_{k\to\infty} d_k = \bar{d} \text{ and } \lim_{k\to\infty} \mathscr{G}(x_k) = \mathscr{G}(\bar{x}) < 0. \tag{4.9}$$

For k large enough,

$$(\mu \circ F_\Omega)(x_k + 2^{-q}d_k) - (\mu \circ F_\Omega)(x_k) < \rho 2^{-q}\mathscr{G}(x_k).$$

This, in view of the definition of μ and step 4 of Algorithm 1, implies that $\tau_k \geq 2^{-q}$ for k large enough. Hence taking into account the second limit in (4.9), we conclude that $\liminf_{k\to\infty} \tau_k |\mathscr{G}(x_k)| > 0$, in contradiction with (4.8). Hence, the result follows. □

Theorem 4.4. *Let U be a nonempty convex open subset of $\mathbb{R}^n$. Take $x \in U$, $\alpha \in \mathscr{P}_x$ and $0 < b$. If $\nabla^2 F(x, \zeta_{\alpha_j}) \leq bI$ for all $j \in [\eta(x)]$, then*

$$|\mathcal{G}(x)| \leq \frac{L}{2b} \| \sum_{j=1}^{[\eta(x)]} \lambda_j \nabla F(x, \zeta_{\alpha_j}) \|^2$$

for all $\lambda_j \geq 0$, with $\sum_{j=1}^{[\eta(x)]} \lambda_j = 1$, where L is the Lipschitz constant of ψ_e.

Proof. Let $\lambda_j \geq 0$ with $\sum_{j=1}^{[\eta(x)]} \lambda_j = 1$ be given. Then, from the definition of $\mathcal{G}$, we have

$$\begin{aligned}
\mathcal{G}(x) &= \min_{(\alpha,d)\in\mathscr{P}_x\times\mathbb{R}^n} \left\{ \max_{j\in[\eta(x)]} \psi_e\big(\nabla F(x,\zeta_{\alpha_j})^\top d + \tfrac{1}{2} d^\top \nabla^2 F(x,\zeta_{\alpha_j}) d\big) \right\} \\
&\geq \min_{(\alpha,d)\in\mathscr{P}_x\times\mathbb{R}^n} \left\{ \sum_{j=1}^{[\eta(x)]} \psi_e\left(\nabla F(x,\zeta_{\alpha_j})^\top d + \tfrac{1}{2} d^\top \nabla^2 F(x,\zeta_{\alpha_j}) d\right) \right\} \\
&\geq \min_{(\alpha,d)\in\mathscr{P}_x\times\mathbb{R}^n} \left\{ \sum_{j=1}^{[\eta(x)]} \left((-L)\|\nabla F(x,\zeta_{\alpha_j})^\top d\| - \tfrac{L}{2}\|d^\top \nabla^2 F(x,\zeta_{\alpha_j}) d\| \right) \right\} \\
&= \min_{(\alpha,d)\in\mathscr{P}_x\times\mathbb{R}^n} \left\{ \sum_{j=1}^{[\eta(x)]} (-L)\|\nabla F(x,\zeta_{\alpha_j})\|\|d\| - \tfrac{L}{2} \sum_{j=1}^{[\eta(x)]} \|\nabla^2 F(x,\zeta_{\alpha_j})\|\|d\|^2 \right\} \\
&\geq \min_{(\alpha,d)\in\mathscr{P}_x\times\mathbb{R}^n} \left\{ \sum_{j=1}^{[\eta(x)]} (-L)\|\nabla F(x,\zeta_{\alpha_j})\|\|d\| - \tfrac{Lb}{2}\|d\|^2 \right\}.
\end{aligned}$$

Since $d \mapsto \sum_{j=1}^{[\eta(x)]} (-L)\|\nabla F(x,\zeta_{\alpha_j})\|\|d\| - \frac{Lb}{2}\|d\|^2$ is a strongly convex function, its minimum is achieved at the unique point where its gradient vanishes, i.e., $\|d\| = -\frac{1}{b}\sum_{j=1}^{[\eta(x)]} \|\nabla F(x,\zeta_{\alpha_j})\|$. This implies that $\mathcal{G}(x) \geq -\frac{L}{2b}\|\sum_{j=1}^{[\eta(x)]} \nabla F(x,\zeta_{\alpha_j})\|^2$. Thus $|\mathcal{G}(x)| \leq \frac{L}{2b}\|\sum_{j=1}^{[\eta(x)]} \lambda_j \nabla F(x,\zeta_{\alpha_j})\|^2$. □

In the following theorems, we analyze the convergence rate of the sequence $\{x_k\}$ generated by the proposed Newton method for UMOPs.

Theorem 4.5. (Superlinear convergence). *Suppose that* Algorithm 1 *generates an infinite sequence for which* $\bar{x}$ *is an accumulation point, and* $\bar{x}$ *is a regular point for* F_Ω*. Suppose that* U *is the neighborhood of* $\bar{x}$ *as described in Lemma 4.1, and there exist* $a,b,\delta,\varepsilon > 0$ *such that*

(i) $aI \le \nabla^2 F(x,\zeta_{\alpha_j}) \le bI$ *for all* $j \in [\eta(x)]$,
(ii) $\|\nabla^2 F(x,\zeta_{\alpha_j}) - \nabla^2 F(y,\zeta_{\alpha_j})\| < \varepsilon$ *for all* $x,y \in U$ *with* $\|x-y\| < \delta$*, and*
(iii) $\varepsilon \le a(1-\rho)$.

Then, the step length $\tau_k = 1$*, after sufficiently large* k*, and* $\{x_k\}$ *converges to* $\bar{x}$ *with superlinear rate.*

Proof. The convergence of sequence $\{x_k\}$ to a stationary point $\bar{x}$ is guaranteed in Theorem 4.3. Since $F(\cdot,\zeta_{\alpha_j})$'s are twice continuously differentiable, we see, for any $\varepsilon > 0$, that there exists $\delta_\varepsilon > 0$ such that

$$B(\bar{x},\delta_\varepsilon) \subset U, \text{ and } \left\|\nabla^2 F(x,\zeta_{\alpha_j}) - \nabla^2 F(y,\zeta_{\alpha_j})\right\| < \varepsilon \ \text{ for all } x,y \in B(\bar{x},\delta_\varepsilon).$$

For $x \in U$, $\lambda_j \ge 0$ and $\sum_{j=1}^{[\eta(x)]} \lambda_j = 1$, suppose

$$\Psi(d,\lambda) = \sum_{j=1}^{[\eta(x)]} \lambda_j \nabla F(x,\zeta_{\alpha_j})^\top d + \tfrac{1}{2}\sum_{j=1}^{[\eta(x)]} \lambda_j d^\top \nabla^2 F(x,\zeta_{\alpha_j}) d.$$

Using Danskin's theorem (see [31, Proposition 4.5.1]), Ψ attains minimum value when

$$\sum_{j=1}^{[\eta(x)]} \lambda_j \nabla F(x,\zeta_{\alpha_j}) + \sum_{j=1}^{[\eta(x)]} \lambda_j \nabla^2 F(x,\zeta_{\alpha_j}) d = 0, \tag{4.10}$$

which implies that

$$\begin{aligned} d &= -\left[\sum_{j=1}^{[\eta(x)]} \lambda_j \nabla^2 F(x,\zeta_{\alpha_j})\right]^{-1} \sum_{j=1}^{[\eta(x)]} \lambda_j \nabla F(x,\zeta_{\alpha_j}) \\ &\le -\left[\sum_{j=1}^{[\eta(x)]} \lambda_j \nabla^2 F(x,\zeta_{\alpha_j})\right]^{-1} \max_{j\in[\eta(x)]} \lambda_j \nabla F(x,\zeta_{\alpha_j}) \\ &\le -\tfrac{1}{a} \max_{j\in[\eta(x)]} \lambda_j \nabla F(x,\zeta_{\alpha_j}). \end{aligned} \tag{4.11}$$

Using Lemma 4.1, we have

$$\|\sum_{j=1}^{[\eta(x_{k+1})]} \lambda_j \nabla F(x_k+d_k,\zeta_{\alpha_j}) - \left[\sum_{j=1}^{[\eta(x_k)]} \lambda_j \nabla F(x_k,\zeta_{\alpha_j}) + \sum_{j=1}^{[\eta(x_k)]} \lambda_j \nabla^2 F(x_k,\zeta_{\alpha_j}) d_k\right]\| \le \varepsilon \|d_k\|,$$

i.e., $\|\sum_{j=1}^{[\eta(x_{k+1})]} \lambda_j \nabla F(x_k+d_k,\zeta_{\alpha_j})\| \le \varepsilon\|d_k\|$

i.e., $\|\max_{j\in[\eta(x_{k+1})]} \lambda_j \nabla F(x_k+d_k,\zeta_{\alpha_j})\| \le \varepsilon\|d_k\|$

i.e., $\|d_{k+1}\| \le \frac{\varepsilon}{a}\|d_k\|$ by using (4.11). (4.12)

As $\{x_k\}$ converges to $\bar{x}$, there exists $k_\varepsilon \in \mathbb{N}$ such that, for all $k \geq k_\varepsilon$, $x_k, x_k + d_k \in B(\bar{x}, \delta_\varepsilon)$. Using Taylor's expansion for $j = 1, 2, \ldots, [\eta(x_k)]$, we have

$$\begin{aligned}
F(x_k + d_k, \zeta_{\alpha_j}) \leq\ & F(x_k, \zeta_{\alpha_j}) + \nabla F(x_k, \zeta_{\alpha_j})^\top d_k + \tfrac{1}{2} d_k^\top \nabla^2 F(x_k, \zeta_{\alpha_j}) d_k + \tfrac{\varepsilon}{2}\|d_k\|^2 \\
\leq\ & F(x_k, \zeta_{\alpha_j}) + \rho\left(\nabla F(x_k, \zeta_{\alpha_j})^\top d_k + \tfrac{1}{2} d_k^\top \nabla^2 F(x_k, \zeta_{\alpha_j}) d_k\right) \\
& + (1-\rho)\left(\nabla F(x_k, \zeta_{\alpha_j})^\top d_k + \tfrac{1}{2} d_k^\top \nabla^2 F(x_k, \zeta_{\alpha_j}) d_k\right) + \tfrac{\varepsilon}{2}\|d_k\|^2 \\
\leq\ & F(x_k, \zeta_{\alpha_j}) + \rho\left(\nabla F(x_k, \zeta_{\alpha_j})^\top d_k + \tfrac{1}{2} d_k^\top \nabla^2 F(x_k, \zeta_{\alpha_j}) d_k\right) \\
& + (1-\rho)\Bigg(- d_k^\top \Bigg(\sum_{j=1}^{[\eta(x_k)]} \lambda_j \nabla^2 F(x_k, \zeta_{\alpha_j}) \Bigg) d_k \\
& + \tfrac{1}{2} d_k^\top \Bigg(\sum_{j=1}^{[\eta(x_k)]} \lambda_j \nabla^2 F(x_k, \zeta_{\alpha_j}) \Bigg) d_k \Bigg) + \tfrac{\varepsilon}{2}\|d_k\|^2 \text{ by using (4.10)} \\
\leq\ & F(x_k, \zeta_{\alpha_j}) + \rho\left(\nabla F(x_k, \zeta_{\alpha_j})^\top d_k + \tfrac{1}{2} d_k^\top \nabla^2 F(x_k, \zeta_{\alpha_j}) d_k\right) - \tfrac{a(1-\rho)}{2}\|d_k\|^2 \\
& + \tfrac{\varepsilon}{2}\|d_k\|^2 \text{ using condition (i)} \\
\leq\ & F(x_k, \zeta_{\alpha_j}) + \rho\left(\nabla F(x_k, \zeta_{\alpha_j})^\top d_k + \tfrac{1}{2} d_k^\top \nabla^2 F(x_k, \zeta_{\alpha_j}) d_k\right) + \tfrac{\varepsilon - a(1-\rho)}{2}\|d_k\|^2.
\end{aligned}$$

Now from condition (iii), we have

$$\varepsilon \leq a(1-\rho) \implies \tfrac{\varepsilon - a(1-\rho)}{2} \leq 0.$$

Then, this allows to take $\tau_k = 1$ for $k \geq k_\varepsilon$. Now, for $k \geq k_\varepsilon$, we have

$$\|x_{k+1} - x_{k+2}\| = \|d_{k+1}\| \leq \tfrac{\varepsilon}{a}\|d_k\| = \tfrac{\varepsilon}{a}\|x_k - x_{k+1}\| \text{ by using (4.12)}.$$

Therefore, if $k \geq k_\varepsilon$ and $j \geq 1$, then

$$\|x_{k+j} - x_{k+j+1}\| \leq (\tfrac{\varepsilon}{a})^j \|x_k - x_{k+1}\|. \tag{4.13}$$

To prove superlinear convergence, we take $0 < \tau < 1$ and define $\bar{\varepsilon} = \min\{a(1-\rho), \frac{\tau}{1+2\tau}a\}$. If $\varepsilon < \bar{\varepsilon}$ and $k \geq k_\varepsilon$, using (4.13) and the convergence of $\{x_k\}$ to $\bar{x}$, we have

$$\|\bar{x} - x_{k+1}\| \leq \sum_{j=1}^{\infty} \|x_{k+j} - x_{k+j+1}\| \leq \sum_{j=1}^{\infty} (\tfrac{\tau}{1+2\tau})^j \|x_k - x_{k+1}\| = \tfrac{\tau}{1+\tau}\|x_k - x_{k+1}\|. \tag{4.14}$$

Hence,

$$\|\bar{x} - x_k\| \geq \|x_k - x_{k+1}\| - \|x_{k+1} - \bar{x}\| \geq \tfrac{1}{1+\tau}\|x_k - x_{k+1}\|. \tag{4.15}$$

Combining the inequalities (4.14) and (4.15), we conclude that if $\varepsilon < \bar{\varepsilon}$ and $k \geq k_\varepsilon$, then

$$\tfrac{\|\bar{x} - x_{k+1}\|}{\|\bar{x} - x_k\|} \leq \tau.$$

As τ is arbitrary in $(0,1)$, we conclude that sequence $\{x^k\}$ converges superlinearly to $\bar{x}$. □

Theorem 4.6. (Quadratic convergence). *Let $\{x_k\}$ be a sequence generated by Algorithm 1 and $\bar{x}$ be one of its accumulation points. Suppose that, in addition to all assumptions of* Theorem 4.5, *$\nabla^2 F(\cdot, \zeta_{\alpha_j})$, for all $j \in [\eta(x)]$, is Lipschitz continuous on U with Lipschitz constant L. Then, $\{x_k\}$ converges quadratically to $\bar{x}$.*

Proof. Using Lemma 4.1, we have

$$\|\sum_{j=1}^{[\eta(x_{k+1})]}\lambda_j\nabla F(x_k+d_k,\zeta_{\alpha_j})-\left[\sum_{j=1}^{[\eta(x_k)]}\lambda_j\nabla F(x_k,\zeta_{\alpha_j})+\sum_{j=1}^{[\eta(x_k)]}\lambda_j\nabla^2 F(x_k,\zeta_{\alpha_j})d_k\right]\|\leq\tfrac{L}{2}\|d_k\|^2$$

i.e., $\|\sum_{j=1}^{[\eta(x_{k+1})]}\lambda_j\nabla F(x_k+d_k,\zeta_{\alpha_j})\|\leq\tfrac{L}{2}\|d_k\|^2$

i.e., $\|\max_{j\in[\eta(x_{k+1})]}\lambda_j\nabla F(x_k+d_k,\zeta_{\alpha_j})\|\leq\tfrac{L}{2}\|d_k\|^2$

i.e., $a\|d_{k+1}\|\leq\dfrac{L}{2}\|d_k\|^2$ by using(4.11)

i.e., $\|d_{k+1}\|\leq\frac{L}{2a}\|d_k\|^2$.

Take $\tau\in(0,1)$. Since $\{x_k\}$ converges superlinearly to $\bar{x}$, there exists k_0 such that, for $k\geq k_0$, $\|\bar{x}-x_{k+1}\|\leq\tau\|\bar{x}-x_k\|$. Therefore, from the triangle inequality, for $l\geq k_0$, we obtain

$$(1-\tau)\|\bar{x}-x_l\|\leq\|x_l-x_{l+1}\|\leq(1+\tau)\|\bar{x}-x_l\|.$$

This implies that

$$\begin{aligned}(1-\tau)\|\bar{x}-x_{k+1}\|\leq\|x_{k+1}-x_{k+2}\|=\|d_{k+1}\|\leq\tfrac{L}{2a}\|d_k\|^2=\tfrac{L}{2a}\|x_k-x_{k+1}\|^2\\ \leq(1+\tau)^2\tfrac{L}{2a}\|\bar{x}-x_k\|^2.\end{aligned}$$

Thus, sequence $\{x_k\}$ converges quadratically to $\bar{x}$. □

5. Numerical Illustration

In this section, we execute the proposed Algorithm 1 through some numerical experiments. The implementation of Algorithm 1, along with the corresponding experimentation, took place using MATLAB R2020a software. This MATLAB software is installed in a Windows 11 laptop with an i5 processor label and 8 GB RAM. To initiate the implementation of the algorithm, we made certain assumptions, outlined as follows.

- We considered the cone C to be a standard ordering cone, that is, $C=\mathbb{R}^2_+$ for all test instances except Example 5.9 and Example 5.10, and the parameter $e=(1,1,\ldots,1)^\top\in\operatorname{int}(C)$ for the scalarizing function ψ_e.
- The parameter ρ in Step 5 for the line search of the Algorithm 1 was chosen $\rho=0.1$.
- The stopping criteria $\|d_k\|<0.001$ was employed, or a maximum number of 100 iterations was reached.
- To estimate the set $\operatorname{Max}(F_\Omega(x_k),C)$ at the k-th iteration in Step 1 of Algorithm 1, we adopted the common method of comparing the elements in $F_\Omega(x_k)$ with upper set order relation.
- At the k-th iteration in Step 2 of Algorithm 1, we compute for every $\alpha\in\mathscr{P}_k$ the unique solution d_a of the strongly convex problem $\min_{d\in\mathbb{R}^n}\mathscr{G}_{x_k}(\alpha,d)$. Then, we find

$$(\alpha_k,d_k)=\operatorname*{argmin}_{\alpha\in\mathscr{P}_k}\mathscr{G}_{x_k}(\alpha,d_a).$$

  with the help of an inbuilt function *fmincon* in MATLAB.

- We formulated and examined various test problems sourced from existing literature of set optimization, incorporating slight modifications alongside introducing new problems. We randomly generated 100 initial points in each case and executed the algorithm. Within the context of each experiment, we have provided a table featuring three columns. The following values have been collected for each test instance:
  - **Initial points:** The value corresponds to the initial column of the table, denoting the count of initial points utilized in solving Algorithm 1 as proposed.
  - **Iterations:** This is a 6-tuple (Min, Max, Mean, Median, Mode, SD) that indicates the minimum, maximum, mean, median, mode, and standard deviation of the number of iterations in those instances reported as solved.
  - **CPU time:** This particular value corresponds to the third column, comprising yet another 6-tuple (Min, Max, Mean, Median, Mode, SD). This tuple shows the minimum, maximum, mean, median, mode, and standard deviation of the CPU time (in seconds) consumed by the initial point in attaining the stopping condition.

Furthermore, for clarity, all the numerical values are displayed for up to four decimal places. In the analysis of each problem, the values of F in (2.2) at every iteration are distinguished by using black and red colours for the initial and final points, respectively. The intermediate points are identified with the colour green. Also, we have used cyan, magenta, and green colours to represent the intermediate points for different initial points.

Example 5.1. Let the uncertainty set be $\Omega = \{0.1, 0.2, \ldots, 3.0\}$. Consider the UMOP with the multi-objective function $F : \mathbb{R}^2 \times \Omega \to \mathbb{R}^2$ defined as

$$F(x,\zeta) = \begin{pmatrix} x_1^2 + x_2^2 + 0.5\sin\left(\frac{2\pi(10\zeta-1)}{60}\right)\cos\left(\frac{2\pi(10\zeta-1)}{60}\right) + 2e^{(x_1+x_2)} \\ 2x_1^2 + 2x_2^2 + 0.5\cos\left(\frac{2\pi(10\zeta-1)}{60}\right) \end{pmatrix}.$$

In Figure 1, various outcomes of Algorithm 1 are illustrated for a selected starting point within the set $[-0.5, 2] \times [-0.5, 0.5]$. Figure 1b and Figure 1a present the sequence of input arguments $\{x_k\}$ and their corresponding outputs $F_\Omega(x_k)$ produced by Algorithm 1, starting from the initial point $x_0 = (1.5, 0.5)^\top$. Moreover, for three randomly selected initial points, the sequence of arguments $\{x_k\}$ and their corresponding outcomes $\{F_\Omega(x_k)\}$ generated by Algorithm 1 (depicted with cyan, magenta, and green colors) are shown in Figure 1d and Figure 1c, respectively.

The performance of Algorithm 1 for Example 5.1 is presented in Table 1.

TABLE 1. Performance of Algorithm 1 on Example 5.1

Number of initial points	Iterations (Min, Max, Mean, Median, Mode, SD)	CPU time (Min, Max, Mean, Median, Mode, SD)
100	(2, 3, 2.6600, 3, 3, 0.4761)	(7.9678, 21.5317, 12.5447, 13.7118, 7.9678, 3.1597)

Below, we introduce three new examples (Example 5.2, Example 5.3, and Example 5.4) in the following manner.

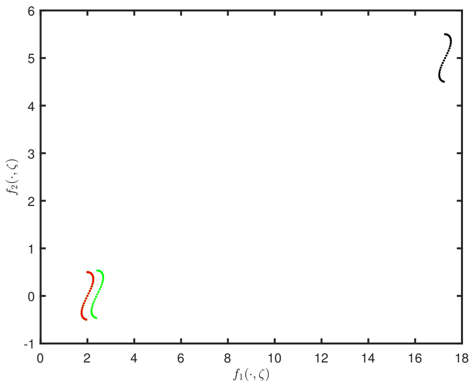

(A) The value of F_Ω at each iteration generated by Algorithm 1 for initial point $x_0 = (1.5, 0.5)^\top$ for Example 5.1

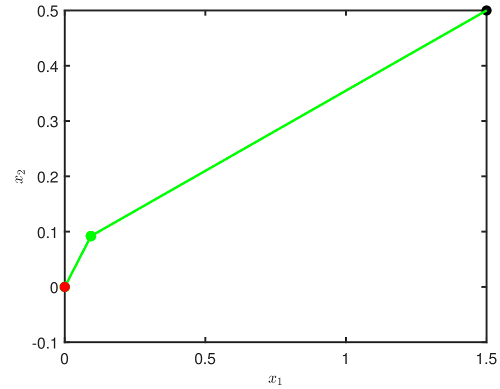

(B) The value of x_k at each iteration generated by Algorithm 1 for initial point $x_0 = (1.5, 0.5)^\top$ for Example 5.1

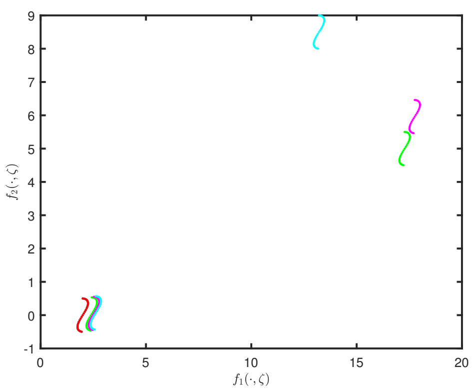

(C) The value of F_Ω at each iteration generated by Algorithm 1 for three different randomly chosen initial points for Example 5.1

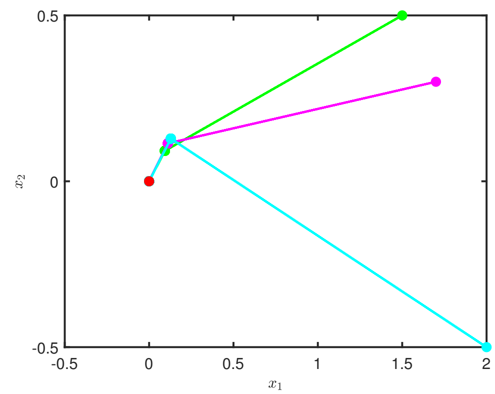

(D) The value of x_k at each iteration generated by Algorithm 1 for three different randomly chosen initial points for Example 5.1

FIGURE 1. Output of Algorithm 1 for Example 5.1

Example 5.2. Let the uncertainty set be $\Omega = \{0.1, 0.2, \ldots, 1.0\}$. Consider the UMOP with the multi-objective function $F : \mathbb{R}^2 \times \Omega \to \mathbb{R}^2$ defined as

$$F(x,\zeta) = \begin{pmatrix} \sin\left(\frac{2\pi(10\zeta-1)}{30}\right) + e^{\frac{x_1^2(10\zeta-1)}{30}}\left((x_1-0.5)^3+(x_2-0.5)^2\right) \\ \cos\left(\frac{2\pi(10\zeta-1)}{30}\right) + e^{\frac{x_2^2(10\zeta-1)}{30}}\left((x_1-0.5)^2+(x_2-0.5)^3\right) \end{pmatrix}.$$

In Figure 2, various outcomes of Algorithm 1 are illustrated for a selected starting point within the set $[0.4, 2.2] \times [0.4, 1.1]$. Figure 2b and Figure 2a present the sequence of input arguments $\{x_k\}$ and their corresponding outputs $F_\Omega(x_k)$ produced by Algorithm 1, starting from the initial point $x_0 = (2.2, 1)^\top$. Moreover, for three randomly selected initial points, the sequence

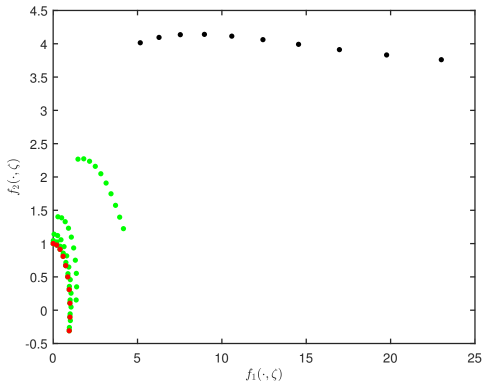

(A) The value of F_Ω at each iteration generated by Algorithm 1 for initial point $x_0 = (2.2, 1.0)^\top$ for Example 5.2

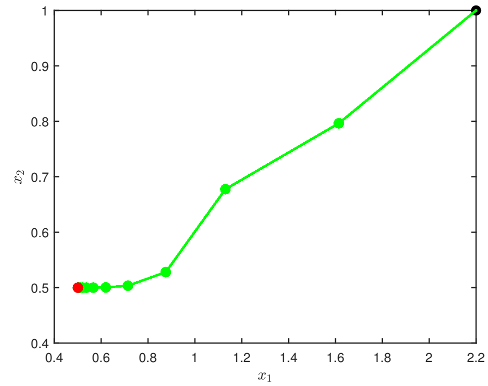

(B) The value of x_k at each iteration generated by Algorithm 1 for initial point $x_0 = (2.2, 1.0)^\top$ for Example 5.2

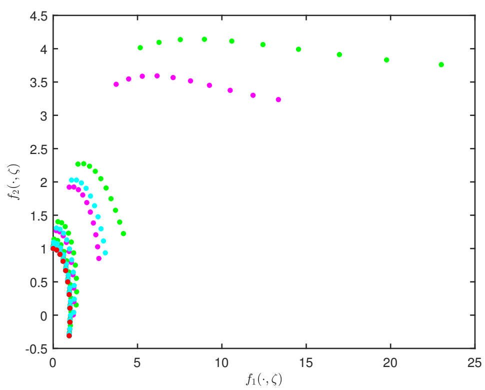

(C) The value of F_Ω at each iteration generated by Algorithm 1 for three different randomly chosen initial points for Example 5.2

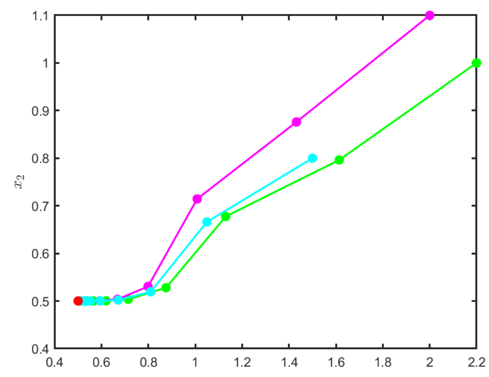

(D) The value of x_k at each iteration generated by Algorithm 1 for three different randomly chosen initial points for Example 5.2

FIGURE 2. Output of Algorithm 1 for Example 5.2

of arguments $\{x_k\}$ and their corresponding outcomes $\{F_\Omega(x_k)\}$ generated by Algorithm 1 (depicted with cyan, magenta, and green colors) are shown in Figure 2d and Figure 2c, respectively. The performance of Algorithm 1 for Example 5.2 is shown in Table 2.

TABLE 2. Performance of Algorithm 1 on Example 5.2

Number of initial points	Iterations (Min, Max, Mean, Median, Mode, SD)	CPU time (Min, Max, Mean, Median, Mode, SD)
100	(1, 13, 12.6200, 13, 13, 0.4878)	(54.4112, 344.4673, 122.2917, 74.7120, 54.4112, 83.9129)

Example 5.3. Let the uncertainty set be $\Omega = \{0.1, 0.2, \ldots, 2.0\}$. Consider the UMOP with the multi-objective function $F : \mathbb{R}^2 \times \Omega \to \mathbb{R}^2$ defined as

$$F(x,\zeta) = \begin{pmatrix} \cos\left(\frac{2\pi x_1(10\zeta-1)}{100}\right)\left(1 + x_1^2 - \sin\left(\frac{4\pi x_2(10\zeta-1)}{100}\right)\right) \\ \sin\left(\frac{2\pi x_2(10\zeta-1)}{100}\right)\left(1 + x_2^2 - \cos\left(\frac{4\pi x_1(10\zeta-1)}{100}\right)\right) \end{pmatrix}.$$

In Figure 3, various outcomes of the Algorithm 1 are illustrated for a selected starting point within the set $[1.2, 1.8] \times [0.9, 1.3]$. Figure 3a depicts the sequence $\{F_\Omega(x_k)\}$ generated by Algorithm 1 for a chosen starting point $x_0 = (1.5, 1.0)^\top$. In Figure 3b, we test our algorithm for three initial points and depict their corresponding output (marked with green, magenta, and cyan colors).

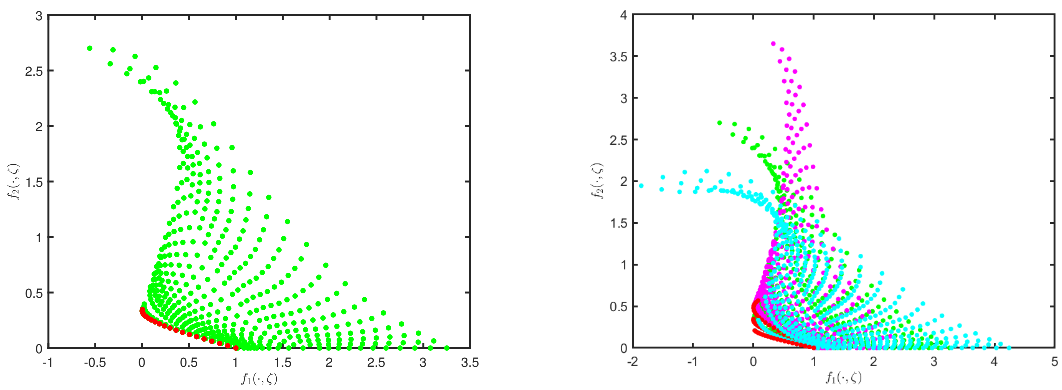

(A) The value of F_Ω at each iteration generated by Algorithm 1 for Example 5.3 for the initial point$x_0 = (1.5, 1.0)^\top$

(B) The value of F_Ω for three different initial points at each iteration generated by Algorithm 1 of Example 5.3

FIGURE 3. Output of Algorithm 1 for Example 5.3

The performance of Algorithm 1 for Example 5.3 is shown in Table 3.

TABLE 3. Performance of Algorithm 1 on Example 5.3

Number of initial points	Iterations (Min, Max, Mean, Median, Mode, SD)	CPU time (Min, Max, Mean, Median, Mode, SD)
50	(1, 10, 5.8400, 6, 6, 1.5167)	(44.0554, 177.0172, 98.3708, 100.6665, 44.0554, 28.1271)

Example 5.4. Let the uncertainty set be $\Omega = \{0.1, 0.2, \ldots, 10.0\}$. Consider the UMOP with the multi-objective function $F : \mathbb{R}^2 \times \Omega \to \mathbb{R}^2$ defined as

$$F(x,\zeta) = \begin{pmatrix} x_1^2 + x_2^2 + 0.5\sin\left(\frac{2\pi(30\zeta-1)}{100}\right) \\ 2x_1^2 + 2x_2^2 + 0.5\cos\left(\frac{2\pi(20\zeta-1)}{100}\right) \end{pmatrix}.$$

In Figure 4, various outcomes of Algorithm 1 are illustrated for a selected starting point within the set $[0, 1.8] \times [0, 1.8]$. For three randomly selected initial points, the sequence of arguments

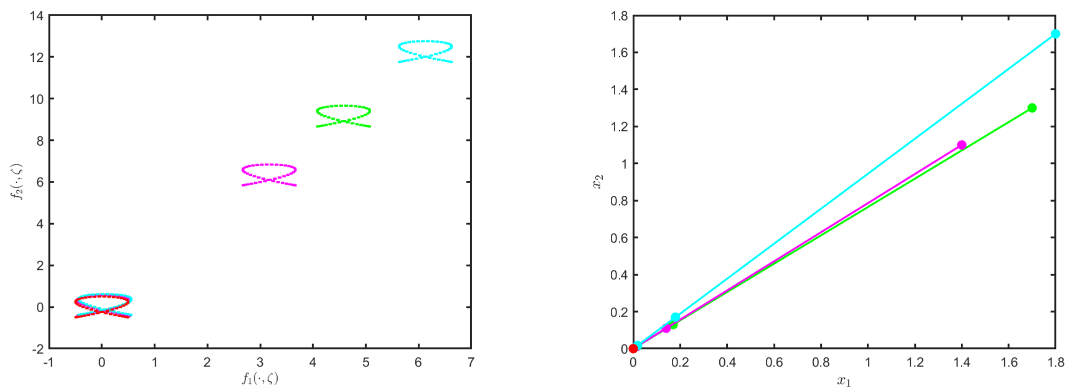

(A) The value of F_Ω for three different initial points at each iteration generated by Algorithm 1 of Example 5.4

(B) The value of x_k at each iteration generated by Algorithm 1 for three different randomly chosen initial points for Example 5.4

FIGURE 4. Output of Algorithm 1 for Example 5.4

$\{x_k\}$ and their corresponding outcomes $\{F_\Omega(x_k)\}$ generated by Algorithm 1 (depicted with cyan, magenta, and green colors) are shown in Figure 4b and Figure 4a, respectively.
The performance of Algorithm 1 for Example 5.4 is shown in Table 4.

TABLE 4. Performance of Algorithm 1 on Example 5.4

Number of initial points	Iterations (Min, Max, Mean, Median, Mode, SD)	CPU time (Min, Max, Mean, Median, Mode, SD)
100	(1, 6, 6, 6, 6, 0)	(31.1872, 43.9398, 37.9914, 40.4395, 31.1872, 4.0770)

Example 5.5. Let the uncertainty set be $\Omega = \{0.1, 0.2, \ldots, 25.0\}$. Consider the UMOP with the multi-objective function $F : \mathbb{R}^2 \times \Omega \to \mathbb{R}^2$ defined as

$$F(x,\zeta) = \begin{pmatrix} 0.35 \sin\left(\frac{2\pi(20\zeta-1)}{250}\right) \cos\left(\frac{2\pi(20\zeta-1)}{250}\right) + x^2 \\ 0.35 \cos\left(\frac{2\pi(30\zeta-1)}{250}\right) + \frac{1}{(1+e^{2x})} + \cos 2x \end{pmatrix}.$$

In Figure 5, various outcomes of the Algorithm 1 are illustrated for a selected starting point within the set $[1.87, 2]$. Figure 5a depicts the sequence $\{F_\Omega(x_k)\}$ generated by Algorithm 1 for a chosen starting point $x_0 = 2$. In Figure 5b, we test our algorithm for three initial points and depict their corresponding output (marked with green, magenta, and cyan colors).

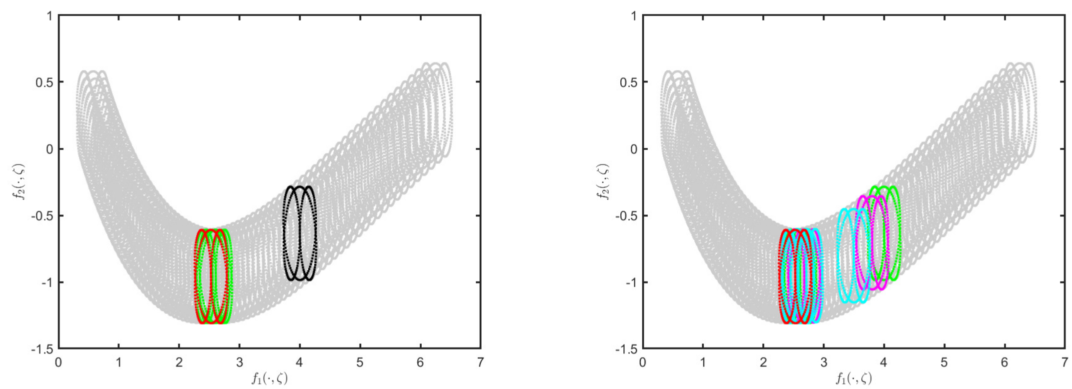

(A) The value of F_Ω at each iteration generated by Algorithm 1 for Example 5.5 for the initial point $x_0 = 2.0$

(B) The value of F_Ω for three different initial points at each iteration generated by Algorithm 1 of Example 5.5

FIGURE 5. Output of Algorithm 1 for Example 5.5

The performance of Algorithm 1 for Example 5.5 is shown in Table 5.

TABLE 5. Performance of Algorithm 1 on Example 5.5

Number of initial points	Iterations (Min, Max, Mean, Median, Mode, SD)	CPU time (Min, Max, Mean, Median, Mode, SD)
100	(1, 5, 3.5400, 5, 5, 1.8609)	(6.5103, 30.8964, 19.9434, 22.4633, 6.5103, 8.9238)

Example 5.6. Let the uncertainty set be $\Omega = \{0.1, 0.2, \ldots, 1.4\}$. Consider the UMOP with the multi-objective function $F : \mathbb{R}^2 \times \Omega \to \mathbb{R}^2$ defined as

$$F(x,\zeta) = \begin{pmatrix} x_1^2 + x_2^2 + 0.25\sin\left(\frac{2\pi(10\zeta-1)}{14}\right) - 0.1\zeta \\ 2x_1^2 + 2x_2^2 + 0.25\cos\left(\frac{2\pi(10\zeta-1)}{14}\right) + 0.2\zeta \\ x_1^2 + x_2^2 + 10\zeta \end{pmatrix}.$$

In Figure 6, various outcomes of Algorithm 1 are illustrated for a selected starting point within the set $[0,2] \times [-0.15, 0.30]$. Figure 6b and Figure 6a presents the sequence of input arguments $\{x_k\}$ and their corresponding outputs $F_\Omega(x_k)$ produced by Algorithm 1, starting from the initial point $x_0 = (2,0)^\top$. Moreover, for three randomly selected initial points, the sequence of arguments $\{x_k\}$ and their corresponding outcomes $\{F_\Omega(x_k)\}$ generated by Algorithm 1 (depicted with cyan, magenta, and green colors) are shown in Figure 6d and Figure 6c, respectively.
The performance of Algorithm 1 for Example 5.6 is shown in Table 6.

TABLE 6. Performance of Algorithm 1 on Example 5.6

Number of initial points	Iterations (Min, Max, Mean, Median, Mode, SD)	CPU time (Min, Max, Mean, Median, Mode, SD)
100	(1, 5, 4.8100, 5, 5, 0.3946)	(33.3476, 49.2138, 41.8439, 43.4114, 33.3476, 3.8975)

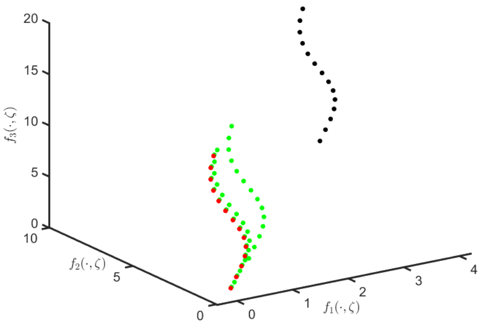

(A) The value of F_Ω at each iteration generated by Algorithm 1 for Example 5.6 for the initial point $x_0 = (2.0, 0.0)^\top$

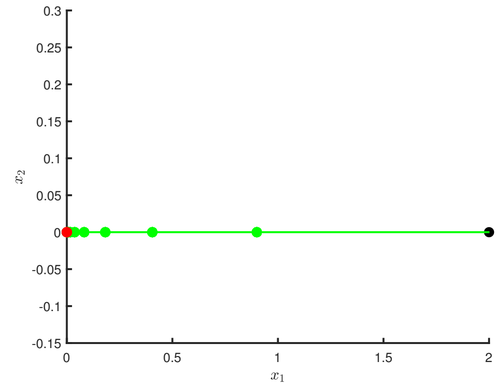

(B) The value of x_k at each iteration generated by Algorithm 1 for initial point $x_0 = (2.0, 0.0)^\top$ for Example 5.6

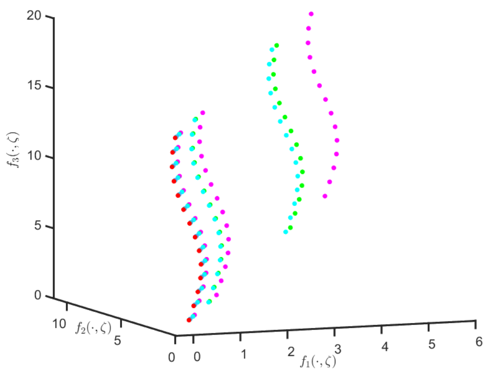

(C) The value of F_Ω for three different initial points at each iteration generated by Algorithm 1 of Example 5.6

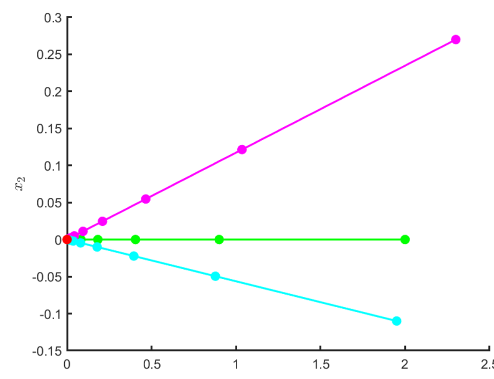

(D) The value of x_k at each iteration generated by Algorithm 1 for three different randomly chosen initial points for Example 5.6

FIGURE 6. Output of Algorithm 1 for Example 5.6

Example 5.7. Let the uncertainty set be $\Omega = \{0.1, 0.2, \ldots, 3.0\}$. Consider the UMOP with the multi-objective function $F : \mathbb{R}^2 \times \Omega \to \mathbb{R}^2$ defined as

$$F(x,\zeta) = \begin{pmatrix} x^2 + \frac{(10\zeta - 1)}{30} \\ (x^2 - 4)\cos\left(x^2 - 4\right) + \frac{(10\zeta - 1)}{30} \\ x^2 \frac{(10\zeta - 1)}{30} \end{pmatrix}.$$

In Figure 7, various outcomes of Algorithm 1 are illustrated for a selected starting point within the set $[2.27, 2.47]$. Figure 7a depicts the sequence $\{F_\Omega(x_k)\}$ generated by Algorithm 1 for a chosen starting point $x_0 = 2.35$. In Figure 7b, we test our algorithm for three initial points and depict their corresponding output (marked with green, magenta, and cyan colors).

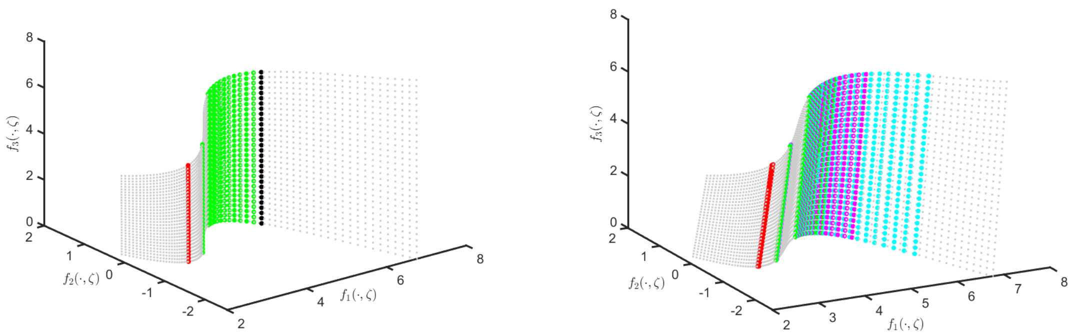

(A) The value of F_Ω at each iteration generated by Algorithm 1 for Example 5.7 for the initial point $x_0 = 2.35$

(B) The value of F_Ω for three different initial points at each iteration generated by Algorithm 1 of Example 5.7

FIGURE 7. Output of Algorithm 1 for Example 5.7

The performance of Algorithm 1 for Example 5.7 is shown in Table 7.

TABLE 7. Performance of Algorithm 1 on Example 5.7

Number of initial points	Iterations (Min, Max, Mean, Median, Mode, SD)	CPU time (Min, Max, Mean, Median, Mode, SD)
100	(1, 23, 8.2500, 5, 5, 6.0509)	(0.5592, 16.1918, 4.9428, 2.1755, 0.5592, 4.4797)

Example 5.8. Consider the UMOP with the multi-objective function $F : \mathbb{R}^2 \times \Omega \to \mathbb{R}^2$ defined as

$$F(x,\zeta) = \frac{1}{2}\begin{pmatrix} \|x - l_1 - \zeta\|^2 \\ \|x - l_2 - \zeta\|^2 \\ \|x - l_3 - \zeta\|^2 \end{pmatrix},$$

where $l_1 = \begin{pmatrix} 0 \\ 8 \end{pmatrix}, l_2 = \begin{pmatrix} 0 \\ 0 \end{pmatrix}$ and $l_3 = \begin{pmatrix} 8 \\ 0 \end{pmatrix}$. We consider a uniform partition set of 10 points of the interval $[-1,1]$ given by

$$\Omega = \left\{ -1, -1 + \tfrac{1}{s}, -1 + \tfrac{2}{s}, \ldots, -1 + \tfrac{2s-1}{s}, 1 \right\} \text{ with } s = 4.5.$$

A scenario $\zeta = (\zeta_1, \zeta_2)$ is an element of the uncertainty set $\Omega \times \Omega$. In Figure 8, a total of 70 initial points were generated in the square $[-50,50] \times [-50,50]$. The grey points represent the set $(l_1 + \zeta) \cup (l_2 + \zeta) \cup (l_3 + \zeta)$ and the locations of l_1, l_2, l_3 are depicted in blue colour. The values of the sequence $\{x_k\}$ generated by Algorithm 1 for three different randomly chosen initial points are given with cyan, magenta, and green colors as shown in Figure 8. The performance of Algorithm 1 for Example 5.8 is shown in Table 8.

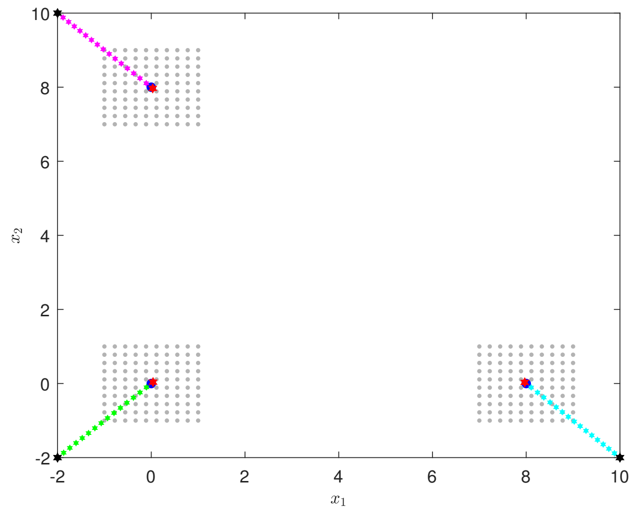

(A) The value of F_Ω for three different initial points at each iteration generated by Algorithm 1 of Example 5.8

FIGURE 8. Output of Algorithm 1 for Example 5.8

TABLE 8. Performance of Algorithm 1 on Example 5.8

Number of initial points	Iterations (Min, Max, Mean, Median, Mode, SD)	CPU time (Min, Max, Mean, Median, Mode, SD)
70	(1, 25, 23.3382, 24, 24, 1.0736)	(19.3772, 396.0796, 111.0618, 88.6105, 19.3772, 88.4447)

Example 5.9. Let the uncertainty set be $\Omega = \{0.1, 0.2, 0.3, 0.4\}$. Consider the UMOP with the multi-objective function $F : \mathbb{R}^2 \times \Omega \to \mathbb{R}^2$ defined as

$$F(x,\zeta) = \begin{pmatrix} 2x^3 + \frac{(10\zeta-3)}{2} + \frac{4x(10\zeta-3)}{2} \\ \frac{x^2}{4}\cos x - \cos^2(x)\frac{(10\zeta-3)}{2} \end{pmatrix}.$$

The cone is C^* given by $C^* = \{(z_1, z_2)^\top \in \mathbb{R}^2 : 15z_1 - 100z_2 \geq 0, -9z_1 + 100z_2 \geq 0\}$.

In Figure 9, various outcomes of the Algorithm 1 are illustrated for a selected starting point within the set $[4.34, 4.7]$. Figure 9a depicts the sequence $\{F_\Omega(x_k)\}$ generated by Algorithm 1 for a chosen starting point $x_0 = 4.7$. It can seen that the points depicted with red color are optimal points of F_Ω as the set $(123.0982, -3.0901)^\top - C^*$ does not contain any element of $F_\Omega(x)$ other than $(123.0982, -3.0901)$ for all $x \in [4.3400, 4.7000]$. In Figure 9b, we test our algorithm for three initial points and depict their corresponding output (marked with green, magenta, and cyan colors).

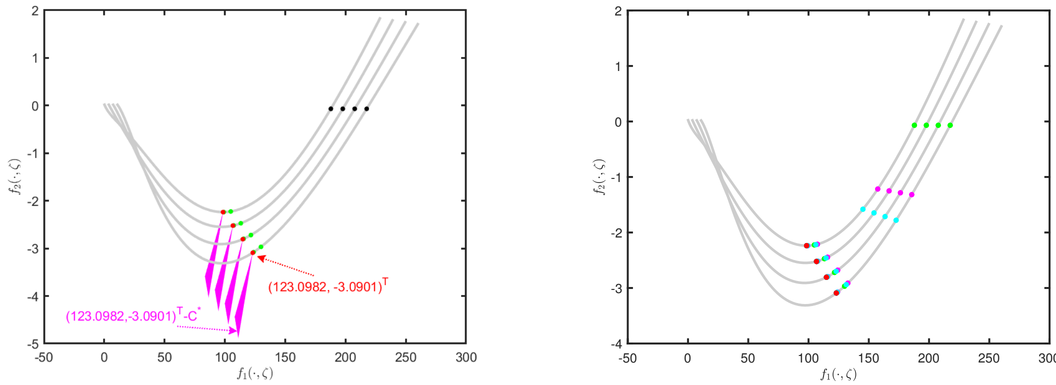

(A) The value of F_Ω at each iteration generated by Algorithm 1 for Example 5.9 for the initial point $x_0 = 4.7000$

(B) The value of F_Ω for three different initial points at each iteration generated by Algorithm 1 of Example 5.9

FIGURE 9. Output of Algorithm 1 for Example 5.9

The performance of Algorithm 1 for Example 5.9 is shown in Table 9.

TABLE 9. Performance of Algorithm 1 on Example 5.9

Number of initial points	Iterations (Min, Max, Mean, Median, Mode, SD)	CPU time (Min, Max, Mean, Median, Mode, SD)
100	(1, 3, 2.9900, 3, 3, 0.1000)	(2.2930, 10.6611, 3.6688, 3.2122, 2.2930, 1.5694)

Example 5.10. Let the uncertainty set be $\Omega = \{0.1, 0.2, \ldots, 1.0\}$. Consider the UMOP with the multi-objective function $F : \mathbb{R}^2 \times \Omega \to \mathbb{R}^2$ defined as

$$F(x,\zeta) = \begin{pmatrix} x_1^2 + x_2^2 + 0.1e^{x_1 x_2} + x_1^2 \cos x_2 + 0.7\cos\left(\frac{2\pi(10\zeta-1)}{200}\right)\sin^2\left(\frac{2\pi(10\zeta-1)}{200}\right) \\ x_1^2 + x_2^2 + 5\log(|x_1 x_2|) + x_2^2\cos x_1 + 25\cos^2\left(\frac{2\pi(10\zeta-1)}{200}\right)\sin^2\left(\frac{2\pi(10\zeta-1)}{200}\right) \end{pmatrix}.$$

In Figure 10, various outcomes of Algorithm 1 are illustrated for a selected starting point within the set $[-0.3, 0.5] \times [-1.2, 0.4]$. For three randomly selected initial points, the sequence of arguments $\{x_k\}$ and their corresponding outcomes $\{F_\Omega(x_k)\}$ generated by Algorithm 1 (depicted with cyan, magenta, and green colors) are shown in Figure 10b and Figure 10a, respectively.

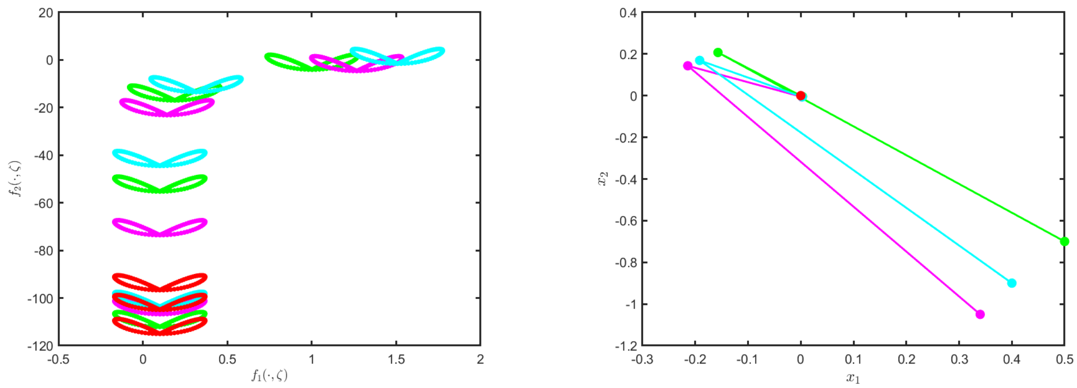

(A) The value of F_Ω for three different initial points at each iteration generated by Algorithm 1 of Example 5.10

(B) The value of x_k at each iteration generated by Algorithm 1 for three different randomly chosen initial points for Example 5.10

FIGURE 10. Output of Algorithm 1 for Example 5.10

The performance of Algorithm 1 for Example 5.10 is shown in Table 10.

TABLE 10. Performance of Algorithm 1 on Example 5.10

Number of initial points	Iterations (Min, Max, Mean, Median, Mode, SD)	CPU time (Min, Max, Mean, Median, Mode, SD)
25	(1, 4, 4, 4, 4, 0)	(190.0765, 234.9737, 210.1367, 209.6842, 190.0765, 9.8043)

6. CONCLUSION

In this paper, we introduced a Newton method to identify weakly robust efficient solutions for UMOPs with an uncertainty set of finite cardinality. We employed a set-valued optimization viewpoint to transform it into a deterministic problem. The deterministic set optimization problem was defined in such a way that the efficient solutions of this problem under upper set-order relation are robust efficient solutions of the considered UMOP. Employing the concept of partition set, we formulated a class of VOPs and we obtained efficient solutions of the set optimization problem, thereby capturing robust efficient solutions of the UMOP. By assuming all vector-valued functions associated with each uncertain scenario to be twice continuously differentiable and locally strong convex, the convergence analysis of the proposed Newton method was derived. It is found that if the weakly robust efficient point satisfies the regularity condition, then the sequence provided by the method locally converges superlinearly (Theorem 4.5), and the Newton step is be a full Newton step. Furthermore, a local quadratic convergence (Theorem 4.6) was identified when the second-order derivatives of the objective functions across all uncertain scenarios are Lipschitz continuous.

The present investigation inspires us to seek weakly robust efficient solutions for UMOPs through the application of Newton's method. Numerous alternative methods (see, e.g., [21, 32, 33, 34, 35]) can be developed for capturing these weakly robust efficient solutions. In future research, we would like to focus on the following directions:

- Develop methods to solve UMOP with infinite or continuous uncertainty sets.
- To examine the complete set of strictly robust efficient, weakly efficient, and efficient solutions for UMOP, one can try to capture a discrete approximation of the complete set.
- Given the practical applications associated with the problems possessing this particular structure, there exists a scope for further research in both the general UMOP context and the extension of our findings to encompass other set order relations.

Acknowledgments
Debdas Ghosh acknowledges research grants, from SERB, India, MATRICS (MTR/2021/000696) and CRG (CRG/2022/001347) to carry out this research work. Nand Kishor expresses gratitude for the financial assistance for his research endeavours by the UGC Senior Research Fellowship, India.

REFERENCES

[1] W. Zhou, F. Wang, A PRP-based residual method for large-scale monotone nonlinear equations, Appl. Math. Comput. 261 (2015), 1-7.
[2] C. Huang, R. Su, J. Cao, S. Xiao, Asymptotically stable high-order neutral cellular neural networks with proportional delays and D operators, Math. Comput. Simul. 171 (2020), 127-135.
[3] A. Ben-Tal, L. EI Ghaoui, A. Nemirovski, Robust Optimization, Princeton University Press, Princeton, 2009.
[4] P. Kouvelis, G. Yu, Easily solvable cases of robust discrete optimization problems, In: Robust Discrete Optimization and Its Applications, Nonconvex Optimization and Its Applications, vol 14, pp. 116–152, Springer, Boston, 1997.
[5] D. Kuroiwa, G. M. Lee, On robust multiobjective optimization, Vietnam J. Math. 40 (2012), 305-317.
[6] M. Ehrgott, J. Ide, A. Schöbel, Minmax robustness for multi-objective optimization problems, Eur. J. Oper. Res. 239 (2014), 17-31.
[7] J. Fliege, R. Werner, Robust multiobjective optimization & applications in portfolio optimization, Eur. J. Oper. Res. 234 (2014), 422-433.
[8] J. Ide, A. Schobel, Robustness for uncertain multi-objective optimization: a survey and analysis of different concepts, OR Spectr, 38 (2016), 235-271.
[9] J. Ide, E. Kobis, Concepts of efficiency for uncertain multi-objective optimization problems based on set order relations, Math. Meth. Oper. Res. 80 (2014), 99-127.
[10] J. Jahn, T. X. D. Ha, New order relations in set optimization, J. Optim. Theory Appl. 148 (2011), 209-236.
[11] G. Eichfelder, J. Jahn, Vector optimization problems and their solution concepts, Recent Developments in Vector Optimization, vol. 1, pp. 1–27, Springer, Berlin, Heidelberg, 2011.
[12] J. Ide, E. Kobis, D. Kuroiwa, A. Schobel, C. Tammer, The relationship between multiobjective robustness concepts and set-valued optimization, Fixed Point Theory Appl. 83 (2014), 1-20.
[13] E. Kobis, A. Sophia, On robust optimization- A unified approach to robustness using a nonlinear scalarizing functional and relations to set optimization, Universitats und Landesbibliothek Sachsen-Anhalt, 2014.
[14] H.Z. Wei, C.R. Chen, S. J. Li, A unified characterization of multiobjective robustness via separation, J. Optim. Theory Appl. 179 (2018), 86-102.
[15] F. Wang, S. Liu, Y. Chai, Robust counterparts and robust efficient solutions in vector optimization under uncertainty, Oper. Res. Lett. 43 (2015), 293-298.
[16] C. Liu, Z. Gong, K. L. Teo, J. Sun, L. Caccetta, Robust multi-objective optimal switching control arising in 1, 3-propanediol microbial fed-batch process, Nonlinear Anal. 25 (2017), 1-20.
[17] G. Eichfelder, C. Kruger, A. Schobel, Decision uncertainty in multiobjective optimization, J. Glob. Optim. 69 (2017), 485-510.
[18] M. Botte, A. Schobel, Dominance for multi-objective robust optimization concepts, Eur. J. Oper. Res. 273 (2019), 430-440.

[19] A. L. Soyster, Convex programming with set-inclusive constraints and applications to inexact linear programming, Oper. Res. 21 (1973), 1154-1157.

[20] A. Ben-Tal, A. Nemirovski, Robust convex optimization, Math. Oper. Res. 23 (1998), 769-805.

[21] S. Kumar, M. A. T. Ansary, N. K. Mahato, D. Ghosh, Y. Shehu, Newton's method for uncertain multiobjective optimization problems under finite uncertainty sets, J. Nonlinear Var. Anal. 7 (2023), 785-809.

[22] G. Bouza, E. Quintana, C. Tammer, A steepest descent method for set optimization problems with set-valued mappings of finite cardinality, J. Optim. Theory Appl. 190 (2021), 711-743.

[23] M. Ehrgott, Multicriteria Optimization, Springer Berlin, Heidelberg, 2005.

[24] A. Göpfert, H. Riahi, C. Tammer, C. Zalinescu, Variational Methods in Partially Ordered Spaces, Springer New York, 2003.

[25] E. Karaman, M. Soyertem, İ. A. Güvenç, D. Tozkan, M. Küçük, Y. Küçük, Partial order relations on family of sets and scalarizations for set optimization, Positivity, 22 (2018), 783-802.

[26] A. A. Khan, C. Tammer, C. Zalinescu, Set-valued optimization, Springer Berlin, Heidelberg, 2014.

[27] D. Kuroiwa, T. Tanaka, T. X. D. Ha, On cone convexity of set-valued maps, Nonlinear Anal. 30 (1997), 1487-1496.

[28] J. Fliege, L. M. G. Drummond, B. F. Svaiter, Newton's method for multiobjective optimization, SIAM J. Optim. 20 (2009), 602-626.

[29] L. M. G. Drummond, F. M. P. Raupp, B. F. Svaiter, A quadratically convergent Newton method for vector optimization, Optimization, 63 (2014), 661-677.

[30] C. Geiger, C. Kanzow, Numerische Verfahren zur Lösung unrestringierter Optimierungsaufgaben, Springer Berlin, Heidelberg, 1999.

[31] D. P. Bertsekas, A. Nedic, A. E. Ozdaglar, Convex Analysis and Optimization, Athena Scientific, 2003.

[32] Jauny, D. Ghosh, Q.H. Ansari, M. Ehrgott, A. Upadhayay, An infeasible interior-point technique to generate the nondominated set for multiobjective optimization problems, Comput. Oper. Res. 155 (2023), 106236.

[33] A. Upadhayay, D. Ghosh, Q.H. Ansari, Jauny, Augmented Lagrangian cone method for multiobjective optimization problems with an application to an optimal control problem, Optim. Eng. 24 (2023), 1633-1665.

[34] Jauny, D. Ghosh, A. Upadhayay, Q.H. Ansari, A trust-region interior-point technique to solve multi-objective optimization problems and its application to a tuberculosis optimal control problem, J. Nonlinear Var. Anal. 6 (2022), 675-691.

[35] K. Kumar, D. Ghosh, A. Upadhayay, J. C. Yao, X. Zhao, Quasi-Newton methods for multiobjective optimization problems: a systematic review, Appl. Set-Valued Anal. Optim. 5 (2023), 291-321.